Master′s Thesis of Science in Agriculture

Fluidized-bed granulation of spray-dried skim milk powder encapsulating *Lactobacillus rhamnosus* GG

유동층 과립기를 이용한 ***Lactobacillus rhamnosus*** **GG**가

포집된 분무건조 탈지분유의 과립화

February 2020

Donghyun Lim

Department of International Agricultural Technology

Graduate School of International Agricultural Technology

Seoul National University

Abstract

The intake of probiotics with health functionalities is now common in everyday life. However, the probiotics encapsulated powder produced by the spray-drying has a low flowability, form a lump at rehydration, and causes a caking at storage due to small particle size and strong cohesive force between particles. Thus, the attempts have been made to overcome these shortcomings by making spray-dried powder into granule using fluidized-bed granulator. But the granulation of spray-dried powder in the fluidized-bed granulator is difficult to proceed due to the strong cohesion between the particles. Furthermore, because the probiotics are encapsulated in powder, it must be run in low temperature to minimize the cell loss during the process.

In this study, the objective is to produce granule of spray-dried microencapsulated powder by conventional fluidized-bed through mixing different powder and moisture-activated dry granulation processes. And measure the effect of granulation to evaluate how much shortcomings of powder has improved by comparing the changes in physicochemical properties of granule and primary powders.

To prepare a spray-dried microencapsulating powder, *Lactobacillus rhamsnosus* GG (LGG) was incubated in the medium containing reconstituted skim milk 10% (w/w), glucose 2% (w/w), yeast extract 1% (w/w), then spray-dried after added more skim milk powder (SMP) to avoid stickiness. Since this spray-dried LGG encapsulated powder (LRP) was not fluidized due to cohesiveness in the fluidized-bed granulator, well-fluidizing SMP was mixed in 50% (w/w). That LRP-SMP mixture showed particle size increase, but particle size distribution was broad and yield was low to 42.8% (w/w). Thus, moisture-activated dry granulation and dehydration were carried out to create sintered bridges between particles of the LRP-SMP mixed in 50:50 (w/w). Through these serial processes, the particle size increased from 33.70 μm to 141.67 μm with almost mono-modal distribution, the cell survivability reached to 80.22%, and yield to 60.78% (w/w). Through scanning electron microscope (SEM), granule with grape grain shaped was also confirmed.

To investigate the effect of granule formation on the change of physicochemical properties of the original particles, moisture content, water activity, dispersibility, flowability / cohesiveness, glass transition temperature, and sticky point temperature were studied. The SMP used as fluidization aid, was also analyzed to correlate its effect on properties of granule. As a result, the water content and water activity of granule did not increase significantly although water as

binder sprayed for whole operation time (15-min, 24% of load mass). And dispersibility in water increased from 49.68% of LRP to 91.64% of granule. The flowability and cohesiveness of LRP were bad and high, respectively, but granule showed fair flowability and intermediate cohesiveness. As a result of the glass transition temperature measurement by differential scanning calorimetry (DSC), the glass transition temperature of granule (69.67 ℃) was higher than LRP (64.16 ℃). And the composition ratio of LRP and SMP in granule was confirmed by using the Couchmann and Karasz (1978) equation substituting the heat capacity change measured at the glass transition; SMP : LRP = 1.08 : 1.

Consequently, LRP was granulated in the fluidized-bed granulator through serial processes of mixing with well-fluidizing SMP, moisture-activated dry granulation, dehydration. Granule resulted in increased yield with high survivability. In addition, granulation improved dispersibility, flowability, and decreased cohesiveness. It also led to an increase in glass transition and sticky point temperature which affects that caking phenomenon during storage.

Keyword : Granulation, Fluidized-bed, Spray drying, *Lactobacillus rhamnosus* GG, Skim milk, Moisture-activated dry granulation, Physicochemical properties.

Student number : 2017-24223

Contents

Chapter 3

Effects of fluidized-bed granulation on the physicochemical properties of particles

List of Tables

Chapter 1

Chapter 2

Chapter 3

List of Figures

Chapter 1

Chapter 2.

Chapter 3.

Chapter 1.

Research background

1. Probiotics

Probiotics are defined as 'live microorganisms which, when administered in adequate amount, confer health benefits to the host' (FAO/WHO, 2002). Probiotics have not been invented but have been in traditional food for a long time like yogurt, cheeses, salty fishes and so on (Amara, 2012). Such probiotics are generally recognized as GRAS (generally recognized as safe). These probiotics also have the following prerequisites; derived from the human body, resistance to stomach acid, bile, and alkali environment of the intestine (Capurso, 2019). Probiotics should also attach to the mucous membranes of the small intestine and be able to metabolic activities (Capurso, 2019). These probiotics (Table 1.1; Kechagia et al., 2013; Amara et al., 2015) have been shown so many health beneficial attributes through numerous scientific and clinical studies (Figure 1.1; Nagpal et al., 2012).

Table 1. 1. Probiotics bacteria, yeast, and mold (Amara et al., 2015; Kechagia et al., 2013)

Bacteria	Species
Lactobacillus	*acidophilus, sporogenes, plantarum, rhamnosus, delbrueckii, reuteri, fermentum, lactus, cellobiosus, brevis, casei, farciminis, paracasei, gasseri, crispatus*
Bifidobacterium	*bifidum, infantis, adolescentis, longum, thermophilum, breve, lactis, animalis*
Streptococcus	*lactis, cremoris, alivarius, intermedius, thermophilis, diacetylactis*
Leuconostoc	*mesenteroides*
Pediococcus	*acidilactici*
Propionibacterium	*freudenreichii*
Bacillus	*cereus var. toyoi*
Enterococcus	*faecalis, faecium*
Yeast and molds	
Saccharomyces cerevisiae, Saccharomyces bourlardii, Aspergillus niger, Aspergillus oryzue, Candida pintolopesii	

1.1. Lactic acid bacteria as probiotics

Among probiotics bacteria strains (Table 1; Kechagia et al., 2013; Amara et al., 2015), lactic acid bacteria (LAB) play important roles in food processing and health maintenance. In particular, these species show various possible health benefits. For example, prevent or decrease the propagation of pathogen microorganisms (Arvola et al., 1999), anti-inflammatory responses (Turcanu et al., 2006), abdominal pain and food allergy, etc (Silva et al., 2014; Montville et al., 2005). Four genera were accepted as LAB: *Lactobacillus, Streptococcus, Leuconostoc,* and *Pediococcus* (Quinto et al., 2014).

Among LAB, particularly *Lactobacillus* species were reported that have physical stress resistance from the environment. They have specific mechanisms for reacting to these stress and environment changes; heat or cold shock, oxidative, acidity, osmotic, high pressure (Serranzanetti et al., 2013). The mechanism for increasing stress resistance comes from the coordinated expression of genes; cell division, membrane composition, DNA metabolism, etc (Serranzanetti et al., 2013). This stress resistance is important for the production and processing of food (e.g. fermentation, spray or freeze-drying, storage, etc).

1.2. *Lactobacillus*

Lactobacillus is one of the LAB strain, and naturally presents in milk. This strain has various functions such as prevention of pathogenic microflora propagation (e.g. lactic acid), enzymes help in digesting some forms of fibers, secreting vitamins (e.g. vitamin B), promotes digestion of food and activates the immune system (Amara et al., 2015, Cammarota et al., 2009). Among *Lactobacillus* strains, *L. rhamnosus* Goldin Gorbach (GG) and *L. acidophilus* are the most and exclusively researched probiotics (Reid et al., 2015; Papizadeh et al., 2016). In particularly, *L. rhamnosus* Goldin Gorbach (GG) has not only been the best researched in detail but also commercialized in the biotechnology industry (Papizadeh et al., 2016). Moreover, its health benefits have been already studied through numerous clinical trails (Gorbach et al., 2017). Furthermore, it has higher heat tolerance than *L. acidophilus* (Ding et al., 2007).

1.3. *Lactobacillus rhamnosus* GG (LGG)

Lactobacillus rhamnosus strain GG (LGG), ATCC 53103 was first isolated from the fecal sample of healthy adult human by Sherwood Gorbach and Barry Goldin (Segers et

al., 2014). The GG is named after a letter from their names. In 1985, it has been found that requirements as probiotics are met; resistance to stomach acid and bile, transfer intestinal epithelial cells while maintaining viability, colonize the intestine with rapid growth rate, antimicrobial production and health beneficial effects (Doron et al., 2005).

LGG is rod shaped, gram-positive bacteria that, when cultured, produces creamy white colony with a distinct buttery odor (Gorbach et al., 2017). It ferments cellobiose, fructose, glucose, mannitol, mannose, melezitose, rhamnose, ribose, saliciin, sorbitol, trehalose, and xylose. It does not ferment the lactose, maltose, sucrose, amygdalin, arabinose, erythritol, glycogen, iniositol, melibiose, or raffinose (Gorbach et al., 2017). An average of 10 to 50 pili of less than 1 μm in length are attached to the LGG cell surface (Tripathi et al., 2013). This allows adhesion to mucus and epithelial cells (Tripathei et al., 2013).

Numerous studies have been conducted on the effects of LGG on human health. The health benefits of LGG in antibiotic, allergy, atopic disease, cancer, cystic fibrosis, cardiovascular diseases, elderly end sport, gastrointestinal infections and diarrhea, irritable bowel syndrome, inflammatory bowel disease, respiratory tract infection, nonalcoholic fatty liver disease, nonalcoholic steatohepatitis, obesity were reported (Capurso et al., 2019; Gorbach et al., 2017).

2. Probiotics encapsulation

Encapsulation is a physicochemical or mechanical process to encapsulate core substance into a protective carrier material with a few nanometers to a few millimeters (Chen et al., 2017). Encapsulation techniques are used in a variety of ways in the food industry: to protect core substance from the environment like oxidation, masking flavors or odors, release control, extend shelf life, etc. The encapsulated core material took the forms of dispersed in the carrier material structure. These carrier materials should be food grade when applied in the food industry and able to protect the core substances: carbohydrate, protein, fats and waxes (Burgain et al., 2011; Chavarri et al., 2012).

Probiotics encapsulation protects the cell against the adverse environment, also controlled release to the desired place in living active state (Burgain et al., 2011).

2.1. Main technologies for probiotics encapsulation

2.1.1. Spray drying

Spray drying is an effective and economical drying method suitable for large-scale industrial applications. In spray drying, the liquid (solution, suspension) is atomized in a vessel using pressure and the solvent evaporates immediately due to contact with hot air or gas (Figure 1.2.; Charvarri et al., 2012).

However high cell loss occurs by exposure to high temperature and osmotic stress due to dehydration during drying. Strain, drying temperature, time and carrier material affects on cell loss during drying (Chavarri et al., 2012). Spray drying is a simple encapsulation technique that can produce and dry microcapsule at once without leaving any solvent residue (Pitigraisorn et al., 2017). As mentioned above, it is an effective, economical encapsulation and drying method, and applicable to industry.

2.1.2. Freeze drying

This technology is also dehydration process by freezing the sample and then reducing surround pressure to sublimate frozen water from solid to the gas phase. This process is carried out by freezing the probiotics and carrier materials together and then vacuuming them to sublimate water (Charvarri et al., 2012). The probiotics survival rate is typically higher than spray drying because the process environment is at lower temperatures (Wang et al., 2004). However, this technology is very expensive than spray drying (Charvarri et al., 2012).

2.1.3. Extrusion

Extrusion is a physical technology of encapsulating probiotics living cells using hydrocolloids as carrier material: alginate and carrageenan, etc. It is a simple and inexpensive encapsulation technology to maintain a high survival rate without damaging probiotics cells (Krasaekoopt et al., 2003). The main drawback of this technology is the slow production of microbeads, making mass production difficult (Burgain et al., 2011).

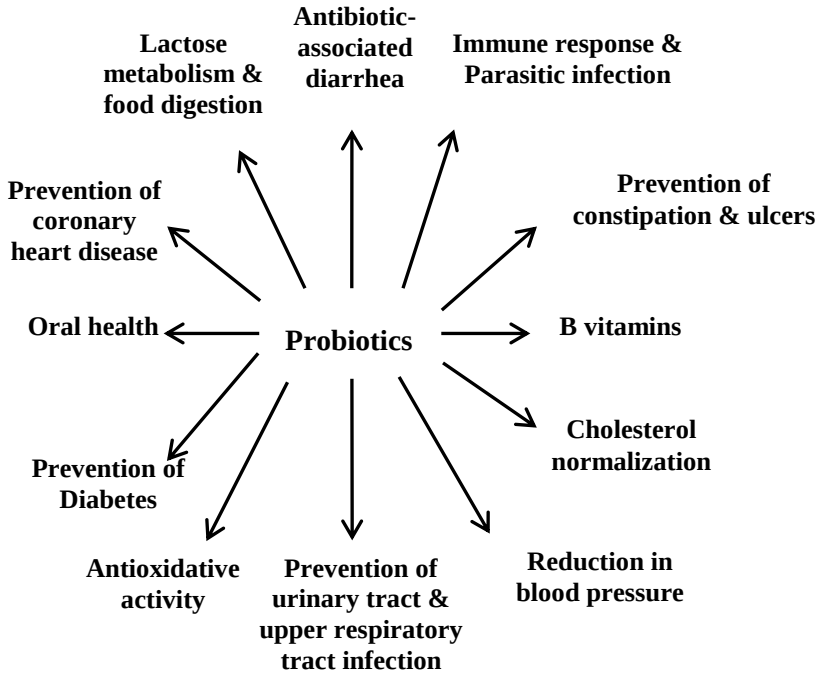

Figure 1.1. Projected prospective health attributes of probiotics (Nagpal et al., 2012)

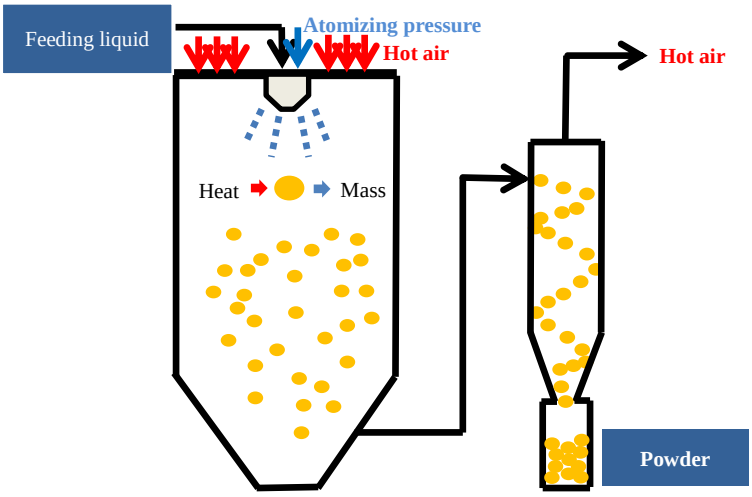

Figure 1.2. Spray drying process

2.2. Carrier materials for probiotics encapsulation

2.2.1. Carbohydrates

Until recently, carbohydrates include trehalose, sorbitol, mannitol, xylose, glucose, sucrose, maltose, lactose, maltodextrin, inulin, galactooligosaccharide, and potato starch were used as encapsulation carrier material during convective droplet drying (Perdana et al., 2014). The low molecular weight and high glass transition temperature procured the higher protection effect in the carbohydrate-rich formulation (Huang et al., 2017).

2.2.2. Proteins

Protein in reconstituted skim milk (RSM) stabilizes cell membrane constituents, preventing cell injury. Besides, it interacts with milk calcium that gives a protective coating on bacterial cell walls (Huang et al., 2016; Zheng et al., 2016). The calcium in milk causes protein aggregation when heat treated which increases the protective effect of *Lb. rhamnosus* GG during convective droplet drying (Wang et al., 2016). Whey has also been reported to have probiotics protection effect during spray-drying (Huang et al., 2016, 2017).

2.3. Encapsulation of LGG by spray drying

2.3.1. Carrier materials for LGG encapsulation by spray drying

The main materials have studied for encapsulating LGG by spray drying were skim milk, protein derived from milk, and adding some carbohydrates or sugars, oils (Table 1.2.)

Table 1.2. Carrier materials for LGG encapsulation by spray drying

Materials (solid concentration)	Air temperature	References
Reconstituted skim milk (20% w/v)	Inlet : 170 ℃ Outlet : 85-90 ℃	Corcoran et al. (2004)
Skim milk (20% w/v) Polydextrose (20% w/v) Inulin (20% w/v) Raftilose® P95 (20% w/v)	Inlet : 140 ℃ Outlet : 70-100 ℃	Ananta et al. (2005)

Whey protein isolate, maltodextrin, glucose, inulin	Inlet : 160 ℃ Outlet : 65 ℃	Ying et al. (2004)
Micellar casein+denatured whey protein (9:1 v/v mixture, total 12.5% w/w)	Inlet : n.a Outlet : 55-85 ℃	Guerin et al. (2017)
WPI (20% w/w), Hylon VII (20% w/w), sun flower oil (40% w/w)	Inlet : 160 ℃ Outlet : 65 ℃	Ying et al. (2010)
WPI (25% w/w), Sugar (25% w/w), Resistant starch (20% w/w), oil (5% w/w)	Inlet : 160 ℃ Outlet : 65 ℃	Ying et al. (2016)
Trehalose (20% w/w)	Inlet : n.a Outlet : 65-70 ℃	Sunny-Roberts, et al. (2009)

n.a : not available

2.3.2. Reconstituted Skim Milk (RSM) as LGG encapsulation material

2.3.2.1. Protective effects of RSM

Reconstituted skim milk (RSM) as a carrier could maintain a greater survival rate of lactic acid bacteria when spray-dried than other carriers tested such as gelatin, maltodextrin, polydextrose and whey permeate (Zheng et al., 2015). In the case of skim milk, milk protein denatured by heat or heat plus calcium ion (Ca^{2+}) increased the resistance of lactic acid bacteria against heat stress (Huang et al., 2014).

2.3.2.2. Adhesion of LGG to milk protein surface

Numerous SpaCBA pill is distributed all around the surface of LGG bacteria cells (Reunanen et al., 2012; Tripath et al., 2012). And long galactose-rich exopolysaccharides (EPS), small glucose-rich EPS (Francius et al., 2009) and other proteins such as MBF (Ossowski et al., 2011) or MabA (Velez et al., 2010) are also distributed. In recent years, adhesive interaction between LGG and whey protein has been confirmed using atomic force microscopy (AFM) (Burgain et al., 2013), particularly with β-lactoglobulin (Guerin et al., 2016). More precisely, the pili on the surface of LGG cell interacts with whey protein and β-lactoglobulin (Reunanen et al., 2012; Guerin et al., 2016). In addition,

pili allow bacteria localized inside the microparticle, increasing the encapsulation rate (Burgain et al., 2014[a], 2014[b]).

3. Limitations of using spray-dried powders

3.1. Small (fine) particle formation

As mentioned above, spray drying (Figure 1.2.) is based on atomization of feeding liquid and evaporation of solvent by convective heat from the droplet. In this atomization, small tiny droplets like aerosol must be formed due to injection by pressure. Thus, the product form from droplet also is small-sized (nano to micron).

Furthermore, the evaporation of solvent during spray drying is described as heat and mass transfer problem (Vehring et al., 2007). The convective heat transfer *(h)* and mass transfer *(m)* coefficients are :

$$h = \frac{Nu \cdot k}{2R} \quad (1)$$

$$m = \frac{Sh \cdot D}{2R} \quad (2)$$

Where *Nu* and *Sh* are corresponding Nusselt and Sherwood number, *k* is heat conductivity of air, *D* is the vapor diffusion coefficient, *R* is the droplet diameter (Julklang et al., 2014; Mezhericher et al., 2008, 2012). As eq (1) and (2), smaller droplet size enhances convective heat and mass transfer coefficient.

For these reasons, the small (fine) particles could be made through spray drying process.

3.2. Cohesiveness of fine particles

Particles are usually divided into bulk solid (d_p > 100 μm), fine (d_p < 100 μm), ultrafine (d_p < 10 μm) and nanoscale (d_p < 100 nm) depending on their size (Tomas et al., 2009). Of these, fine powders, smaller than 100 μm, show problematic characteristics, especially the flowability (Tomas et al., 2009). This is due to van der Waals forces attraction between particles in exceeding the gravitational forces (Tomas et al., 2009). This flow problem (cohesiveness) is critical in many industrial applications, especially

pharmaceutical, food, chemical as well as in mechanical and plant engineering (Tomas et al., 2009). Also, this cohesiveness negatively effects on solubility of the particle (Martini et al., 1999). As a result, improving the flowability of powder has been an important challenge in research and industrial applications during recent decades (Tomas et al., 2009).

4. Granulation

According to Tardos, "Granulation is a part procedure with little fine particle be agglomerate in bigger entity call granule. Fine particles with covering be complete towards get better flow, appear with combination property, towards let pass dustiness also decrease separation, towards any reduce unwanted property otherwise getting better the chemical and physical property of fine powders." (Shanmugam, 2015). As a result, granulation is a technology of particle enlargement that transform small particle into large agglomerate called granule (Shanmugam, 2015). Through the granulation process (Shanmugam, 2015), the followings could be achieved

1. Density increase (occupies a small volume per weight ratio for better transportation and storage)
2. Providing benefit to metering or volumetric dispensing
3. Reducing scattered dust during process
4. Changing the appearance of the product
5. Improving flowability, solubility

Granulation is divided into two types: wet granulation using binder liquid and dry granulation without liquid (Bhattacharjee et al., 2016).

4.1. Wet granulation

The most commonly used granulation process is wet granulation. The wet granulation is a wet massing process of powder blend with binder liquid. Wet granulation techniques include high shear mixer granulation, fluidized-bed granulation, extrusion-spheronization, spray drying, moisture-activated dry granulation (Thejaswini et al., 2013; Shanmugam, 2015).

4.2. Dry granulation

Dry granulation is a process of compressing a powder mixture without using heat or liquid. Two processes are used for dry granulation. The most common method is slugging, where the powder is compressed into a tablet and then milled to yield the granules (Thejaswini et al., 2013). The other method is to compress the powder with a rolling machine (Thejaswini et al., 2013).

5. Fluidized-bed granulation

A fluidized-bed or air-suspension process is used for wet granulation, drying and coating (Bhattacharjee et al., 2016). This process consisted of two consecutive steps. The first step is that the fluidized-bed particles are wetted by sprayed liquid, and agglomerated by liquid bridges. The second step is the formation of solid bonds through drying of liquid bridges (Figure1.3; Figure1.4; Pont et al., 2001).

5.1. Advantages and disadvantages of fluidized-bed process

Advantages of fluidized-bed were, uniform temperature distribution through intensive particle mixing; large solid-gas exchange area; high heat transfer coefficient (Werther, 2005).

Disadvantages of fluidized-bed were, particle erosion and attrition; defluidization as particle agglomeration proceeds; difficult to scale up.

6. Geldart classification of powder

Geldart provides a standard for predicting the fluidization behaviors depends on the Sauter mean particle size, d_p, and the particle density, ρ_s. Based on this standard, particles are classified into 4 groups : A, B, C, D (Table 1.3; Cocco et al., 2014; Geldart, 1973).

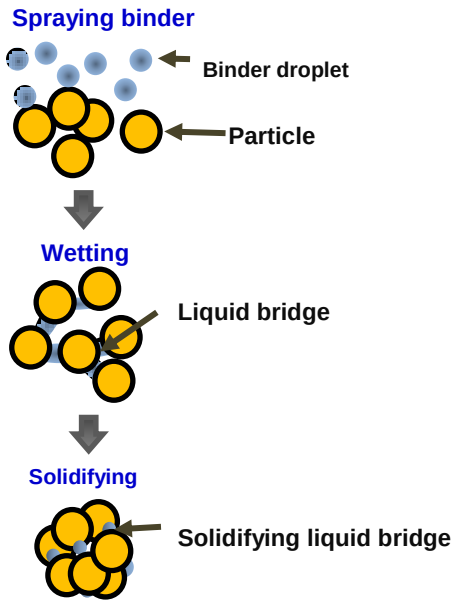

Figure 1.3. Mechanism of fluidized-bed granulation

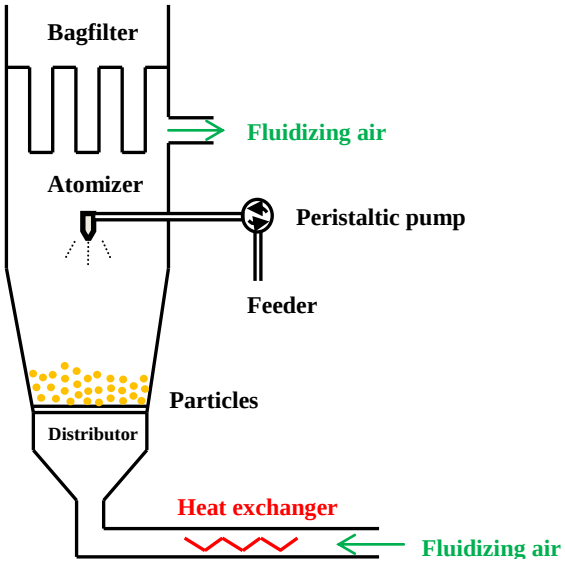

Figure 1.4. Fluidization in a fluidized-bed

Table 1.3. Particle properties of each Geldart group

Properties / Group	A (aeratable)	B (sand-like)	C (fine)	D (large)
Particle diameter (d_p, μm)	30-100	$40 < d_p < 500$	< 20	> 1400
Density (ρ_s, kg/m^3)	< 1400	$1400 < \rho_s < 4000$	< 1400	> 1400
Bed expansion	Large	Small	No expansion	Spouted

These groups of particle shows different fluidization characteristics in the conventional fluidized-bed granulator (Figure 1.5.).

① Geldart group A

Particles are aeratable and well fluidized.

② Geldart group B

Particles do not fluidized smoothly. And very large bubbles are formed.

③ Geldart group C

The most difficult to fluidize. These particles are considered to be cohesive and almost always cause significant channeling phenomenon (i.e. formation of the channel by fast-moving air that bypasses most of particles) during fluidization. Particles of this size behave as cluster rather than individually.

④ Geldart group D

The largest-sized particles belong to this group. The fluidization of these particles requires a large amount of gas. Thus, this group particles show spouting behavior at fluidized. The spouting behavior is the gas moving primarily through the center of the bed.

7. Methods for fluidizing Geldart group C particles

As mentioned above, this group particle is difficult to be fluidized due to attractive inter-particle force (e.g. van der Waals, electrostatic) is greater. There are several methods to improve the fluidizing behavior of these cohesive particles, such as vibration, acoustic field,

magnetic field, adding particles, etc (Table 1.4.). Unlike other methods, mixing different group particles has the advantage that no additional equipment or device is required (Zhou et al., 1999).

Table 1.4. Fluidization methods for Geldart group C particles

Fluidization method	Group C particle	Equipment or mixed particle (d_p)	Reference
Mixing	SiC (4.99 – 13.26 μm)	SiO_2 CLC catalyst FCC catalyst	Zhou et al. (1999)
	Silicon-F (3.7 μm) Silicon Nitrate-F (0.49 μm)	Silicon -L (330 μm) Silicon Nitrate -L (370 μm)	Liu et al. (1993)
Magnetic field	SiO_2 (12 nm)	Magnetic particles Electromagnetic coil	Yu., et al. (2005)
Acoustic field	Zeolite catalyst (13 – 18 μm)	Loud speaker Signal generator	Russo et al. (1995)
Vibration	Glass beads (6 – 10 μm)	Vibration motor	Mawatari et al. (2002)

8. Moisture-activated dry granulation

Moisture-activated dry granulation has the same mechanism as conventional wet granulation. The main differences are the amount of binder liquid used and the level of agglomeration formed. In conventional wet granulation, more binder liquid is used to form larger and wetter granules. And the, remove the excess binder liquid by heat drying and reduce the size of granule by milling (Ullah et al., 2010). However in moisture-activated dry granulation, only a small amount of water is used to make granule, followed by moisture distribution and adsorption. And no heat drying or milling is required. This is because the amount of water used in moisture-activated dry granulation is small, usually 1-4% of entire formation (Gupta et al., 2015; Ullah et al., 2010)

8.1. Mechanism of moisture-activated dry granulation

All or part of the components is mixed to obtain a uniform mixture. Spray a small amount of water (1-4%) onto the powder mixture; Water droplets hydrate the dry particle and form tacky nuclei or tacky wet mass. The binder functions in the rotating states by the impeller or blades of mixer. Then, dry particles adhere to the tacky nuclei or mass to make moist granules. As a result, the granules are small and spherical because very little

water used compared to conventional wet granulation (Figure 1.6; Gupta et al., 2015; Sharma et al., 2017).

The moisture of granule moves from the surface of the first wetted particle to dry surface of the adhered particle, so that excess moisture dispersing and relatively drying effect occurs (Figure 1.7.).

8.2. Advantages and disadvantages of moisture-activated dry granulation.

Advantages of moisture-activated dry granulation were, produce relatively small and narrow size distribution granule with good flowability; applicable to scale up with no or few risks; Low energy consumption without additional drying and milling (Gupta et al., 2015).

Disadvantages of moisture-activated dry granulation were, in special cases (e.g. phase transition), a large amount of water (e.g. more than 5-10%) is required; use of water is a labile component.

8.3. Previous studies on moisture-activated dry granulation

The moisture-activated dry granulation was carried out using a small proportion of binder with impeller mixing for pharmaceutical active compounds (Table 1.5.).

Table 1.5. Previous studies on the moisture-activated dry granulation

Active compounds	Binders	Conditions	References
Acetaminophen Povidone K12 Maltodextrin DE16	Water (2% w/w)	Impeller - 700 rpm, 5 min	Moravkar et al. (2016)
Lactose monohydrate Calcium hydrogen phosphate Povidone K15 Copovidone Guar gum Xanthan gum Microcrystalline cellulose	Water (n.a.)	Impeller - 380 rpm, 2 min	Ochoa-Andrade et al.(2018)
Lactose monohydrate Polyvidone	Water 2% (w/w)	Impeller - 500 rpm, 2 min	Takasaki et al. (2013)

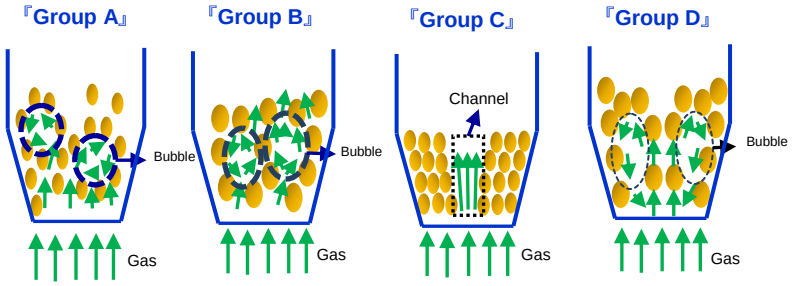

Figure 1.5. Fluidization behavior of particles of Geldart group A, B, C, and D

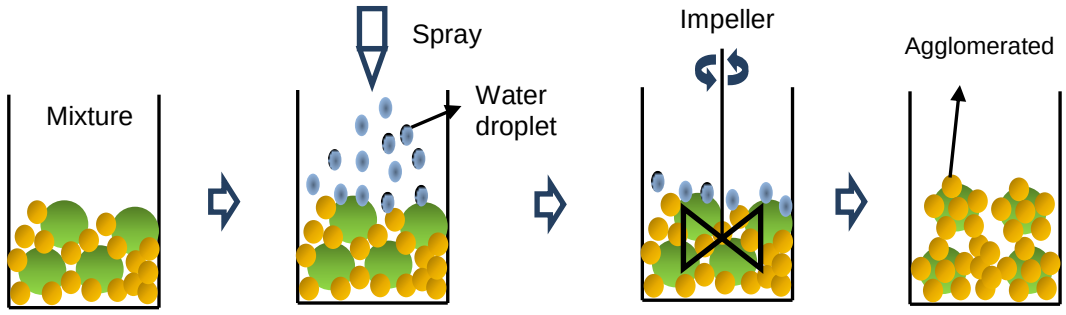

Figure 1.6. Schematic of moisture-activated dry granulation process

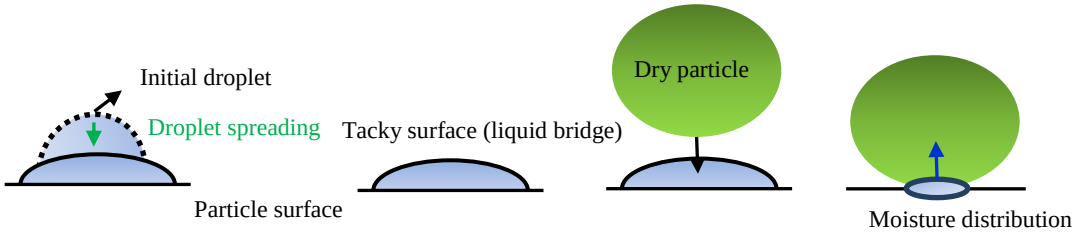

Figure 1.7. Mechanism of moisture-activated dry granulation

9. Research significance

Conventional fluidized-bed granulator has an advantage that formation and drying of granule happen almost at the same time with high heat transfer rate. However, little works on the conventional fluidized-bed granulation of food powders encapsulating probiotics were achieved. Particularly, in the case of fine particle (like spray-dried), there were several difficulties to granulate using a conventional fluidized-bed granulator because fine particles were not fluidized due to its cohesiveness, and should be in low temperature during process due to probiotics cell loss. Furthermore, such cohesiveness causes several disadvantages like poor flowability, lump formation when rehydrated and caking during storage. Therefore, through granulation of this cohesive powder encapsulating probiotics by using fluidized-bed granulator in low temperature, it is possible to compensate for these disadvantages and efficiently produce granule with diminished cell loss.

10. Overall objectives

The overall objective of this study is overcoming the disadvantages of spray-dried LGG encapsulated fine powder by fluidized- bed granulation. To achieve the objective, firstly, produce microencapsulated granule by conventional fluidized-bed through mixing different groups of powder and moisture-activated dry granulation. Secondly, measure the effect of granulation by comparing the changes in physicochemical properties of granule and primary powders.

Thus, chapter 2 describes the process of granulation of spray-dried LGG encapsulated fine powder with fluidized-bed granulator in several steps. Chapter 3 quantifies how granule formation changes the characteristics or disadvantages that it originally had (Figure 1.8.).

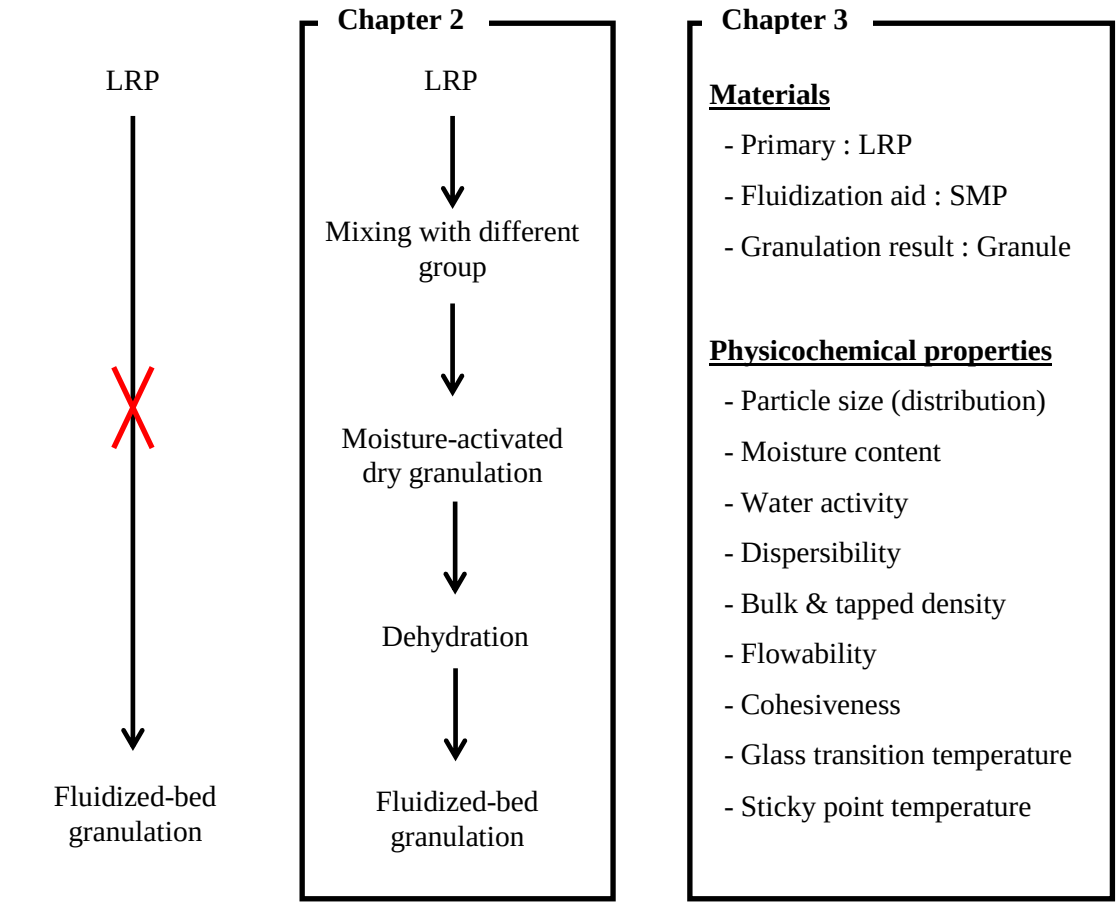

Figure 1.8. Research strategy

Chapter 2.

Fluidized-bed granulation of spray-dried skim milk powder encapsulating *Lactobacillus rhamnosus* GG

1. Introduction

Probiotics are defined as 'live microorganisms which, when administered in adequate amount, confer health benefits to the host' (FAO/WHO, 2002). Probiotics have not been invented but have been in traditional food for a long time like yogurt, cheeses, salty fishes and so on (Amara, 2012). These probiotics have been shown so many health beneficial attributes through numerous scientific and clinical studies like constipation, diarrhea, diabetes, immune response, reduction in blood pressure, etc. (Nagpal et al., 2012). Among probiotics bacteria strains, lactic acid bacteria (LAB) play an important role in food processing and health maintenance. In particular, these species show various possible health benefits. For example, prevent or decrease the propagation of pathogen microorganisms (Arvola et al., 1999), anti-inflammatory responses (Turcanu et al., 2006), abdominal pain and food allergy, etc (Silva et al., 2014; Montville et al., 2005). Four genera were accepted as LAB: *Lactobacillus, Streptococcus, Leuconostoc,* and *Pediococcus* (Quinto et al., 2014). In LAB, particularly *Lactobacillus* species were reported that have physical stress resistance from the environment. They have specific mechanisms for reacting to these stress and environment changes; heat or cold shock, oxidative, acidity, osmotic, high pressure (Serranzanetti et al., 2013). This stress resistance is important for the production and processing of food (e.g. fermentation, spray or freeze-drying, storage, etc).

Lactobacillus, one of the LAB strains, is naturally present in milk. This strain has various functions such as prevention of pathogenic microflora propagation (e.g. lactic acid), enzymes help in digesting some forms of fibers, secreting vitamins (e.g. vitamin B), promote digestion of food and activate the immune system (Amara et al., 2015, Cammarota et al., 2009). In particularly, *L. rhamnosus* Goldin Gorbach (GG) has not only been the best researched in detail, but also commercialized in the biotechnology industry (Papizadeh et al., 2016). Moreover, its health benefits have been already studied through numerous clinical trails (Gorbach et al., 2017).

Lactobacillus rhamnosus strain GG (LGG), ATCC 53103 was first isolated from the fecal sample of healthy adult human by Sherwood Gorbach and Barry Goldin. LGG is rod shaped, gram-positive bacteria that, when cultured, produce creamy white colony with a distinct buttery odor (Gorbach et al., 2017). It ferments cellobiose, fructose, glucose, mannitol, mannose, melezitose, rhamnose, ribose, salicin, sorbitol, trehalose, and xylose. It does not ferment the

lactose, maltose, sucrose, amygdalin, arabinose, erythritol, glycogen, inositol, melibiose, or raffinose (Gorbach et al., 2017). An average of 10 to 50 pili of less than 1 μm in length are attached to the LGG cell surface (Tripathi et al., 2013). This allows adhesion to mucus and epithelial cells (Tripathei et al., 2013). Numerous studies have been conducted on the effects of LGG on human health. The health benefits of LGG in antibiotic, allergy, atopic disease, cancer, cystic fibrosis, cardiovascular diseases, elderly end sport, gastrointestinal infections and diarrhea, irritable bowel syndrome, inflammatory bowel disease, respiratory tract infection, nonalcoholic fatty liver disease, nonalcoholic steatohepatitis, obesity were reported (Capurso et al., 2019; Gorbach et al., 2017).

Encapsulation is a physicochemical or mechanical process to encapsulate core substance into a protective carrier material with a few nanometers to a few millimeters (Chen et al., 2017). Probiotics encapsulation protects the cell against the adverse environment, also controlled release to the desired place in living active state (Burgain et al., 2011). Spray drying is a simple encapsulation technique that can produce and dry microcapsule at once without leaving any solvent residue (Pitigraisorn et al., 2017). Spray drying is an effective and economical drying method suitable for large-scale industrial applications. In spray drying, the liquid (solution, suspension) is atomized in a vessel using pressure and the solvent evaporates immediately due to contact with hot air or gas (Charvarri et al., 2012). Reconstituted skim milk (RSM) as a carrier could maintain a greater survival rate of lactic acid bacteria when spray-dried than other carriers tested such as gelatin, maltodextrin, polydextrose, and whey permeate (Zheng et al., 2015). In the case of skim milk, milk protein denatured by heat or heat plus calcium ion (Ca^{2+}) increased the resistance of lactic acid bacteria against heat stress (Huang et al., 2014). And the pili on the surface of *lactobacillus rhamnosus* GG cell interacts with whey protein and β-lactoglobulin (Reunanen et al., 2012; Guerin et al., 2016). In addition, pili allow bacteria localized inside the microparticle, increasing the encapsulation rate (Burgain et al., 2014).

As mentioned above, spray drying is based on the atomization of feeding liquid and evaporation of solvent by convective heat from droplet. In this atomization, small tiny droplets like aerosol must be formed due to injection by pressure. Thus, the product form from droplet also is small-sized (nano to micron). Furthermore smaller droplet size enhances convective heat and mass transfer coefficient. For these reasons, the small (fine) particles could be made through the spray drying process.

These fine powders, smaller than 100 μm, show problematic characteristics, especially the flowability (Tomas et al., 2009). This is due to van der Waals forces attraction between

particles in exceeding the gravitational forces (Tomas et al., 2009). This flow problem (cohesiveness) is critical in many industrial applications, especially pharmaceutical, food, chemical as well as in mechanical and plant engineering (Tomas et al., 2009). Also, this cohesiveness negatively effects on solubility of the particle (Martini et al., 1999). As a result, improving the flowability of powder has been an important challenge in research and industrial applications during recent decades (Tomas et al., 2009).

Granulation is a technology of particle enlargement that transforms small particles into large agglomerate called granule (Shanmugam, 2015). Through granulation, many disadvantages of fine powder can be overcome such as increase density, reduction of scattered dust, improve flowability and solubility, etc (Shanmugam, 2015).

The most commonly used granulation process is wet granulation. The wet granulation is a wet massing process of powder blend with binder liquid. A fluidized-bed or air-suspension process is used for wet granulation, drying and coating (Bhattacharjee et al., 2016). This process consisted of two consecutive steps. The first step is that the fluidized-bed particles are wetted by sprayed liquid, and agglomerated by liquid bridges. The second step is the formation of solid bonds through drying of liquid bridges (Pont et al., 2001).

However, Geldart group C particles are difficult to be fluidized due to attractive inter-particle force (e.g. van der Waals, electrostatic) is greater. There are several methods to improve the fluidizing behavior of these cohesive particles, such as vibration, acoustic field, magnetic field, adding particles, etc. Unlike other methods, mixing different group particles has the advantage that no additional equipment or device is required (Zhou et al., 1999).

Moisture-activated dry granulation has the same mechanism as conventional wet granulation. The main differences are the amount of binder liquid used and the level of agglomeration formed. In conventional wet granulation, more binder liquid is used to form larger and wetter granules. And the, remove the excess binder liquid by heat drying and reduce the size of a granule by milling (Ullah et al., 2010). However in moisture-activated dry granulation, only a small amount of water is used to make granule, followed by moisture distribution and adsorption. And no heat drying or milling is required. This is because the amount of water used in moisture-activated dry granulation is small, usually 1-4% of entire formation (Ullah et al., 2010; Gupta et al., 2015)

In this study, the objective is to produce microencapsulated granule by conventional fluidized-bed through mixing different groups of powder and moisture-activated dry granulation.

2. Materials and methods

2.1. Materials

Lactobacillus rhamnosus GG, ATCC53103 was provided by Chungbuk National University (Cheongju, Korea). Skim milk powder (Seoul Milk Co. Ltd., Seoul, Korea) was used for culture, spray-drying and fluidization aid. Man Rogosa and Sharp (MRS) broth (Difco, Detroit, MI, USA), glucose (Ducksan, Ansan, Korea), yeast extract (Thermo Fisher Scientific, Erembodegem, Belgium) were used for culture.

2.2. Preparation of LGG-fermented RSM

LGG were sub-cultured sequentially for 24 h, 18 h at 37 ℃ in de Man Rogosa and Sharp (MRS) broth. The reconstituted skim milk (RSM) medium 190 mL was composed of 10% (w/w) skim milk powder, 2% (w/w) glucose, 1% (w/w) yeast and distilled water. To sterilize, heat-treatment was carried out using a water bath (BS-31, Jeiotech, Seoul, Korea) at 90 ℃ for 30 min. After that, LGG was inoculated into the heat-treated RSM and incubated in 42 ℃ water bath with 100 rpm shaking until pH reached to 3.9. After storing in a 1℃ refrigerator to cool it down for overnight.

2.3. Spray drying of LGG-fermented RSM

Skim milk powder (SMP; drying aid for prevention of stickiness) 58 g was added into LGG-fermented RSM and stirred it with a magnetic stirrer for 30 min. This LGG-fermented RSM was fed into the spray dryer (Eyela LRP-1000, Tokyo Rikakikai Co., Tokyo, Japan) using the peristaltic pump. This spray dryer equipped 0.7 mm diameter single nozzle with a concurrent airflow system. The operating conditions were maintained at inlet temperature 160 ± 1 ℃, outlet temperature 80 ± 1 ℃ with feed rate of 300 mL/h, atomization pressure 100 kPa and air flow rate 0.20 – 0.24 m^3/min. The following granulation was carried out with this LGG-fermented reconstituted skim milk powder (LRP).

2.4. Granulation of spray-dried powder by fluidized-bed

2.4.1. Mixing LRP with SMP

LRP and SMP were put in different ratios (90:10, 70:30, 60:40, 50:50 w/w) in a 500 mL beaker, and then mixed by impeller at 500 rpm for 5 min in room

temperature. As a result of granulation, the proportion with the largest change of particle size was selected.

2.4.2. Moisture-activated dry granulation

Sprayed 2.5% w/w distilled water on the surface of LRP and SMP 50:50 (w/w) mixture with commercial hand sprayer. Then re-mixed with the impeller at 500 rpm for 5 min at room temperature. Wait 10 min until contact angle was low enough, and filtered through 1mm sieve to remove the large-sized mass (Figure 2. 1). After the moisture-activated dry granulation, the change in particle size distribution was confirmed.

2.4.3. Dehydration

Moisture-activated dry granulation processed mixture 50 g was dried with a fluidized-bed granulator (BD-600S, IREA Tech Co. Ltd., Daejeon, Korea) at 50 ℃ inlet temperature and 150 L/min air flow rate for 30 min. During drying, 1 g of sample was taken every 5 mins to measure the change in viable cell count, moisture content, water activity. Thus, drying time without affecting viable cell count and no particle attrition was selected.

2.4.4. Fluidized-bed granulation

At all steps (Figure 2.2.), the results were granulated through a top sprayed fluidized-bed granulator (BD-600S, IREA Tech Co. Ltd., Daejeon, Korea; Figure 1.4.). Sample 50 g was placed inside the chamber, and the distilled water as a binder was sprayed at a pressure of 1.1 bar (110 kPa) at 0.8 mL/min using the peristaltic pump while maintaining an inlet temperature 50 ℃ and airflow rate 150 L/min. The operating time was 8 min.

2.5. Particle size analysis

Laser diffraction particle size analyzer (1190LD, CILAS, Orleans, France) was used to analyze the volume-weight mean diameter ($d_{4,3}$) and particle size distribution of particles based on Fraunhofer theory. The number, size, and volume of each peak in the particle size distribution were analyzed.

2.6. Density measurement

True density (kg/m^3) was measured using a gas pycnometer (Ultrapyc1200e, Quantachrome Instrument, Boynton Beach, FL, USA) from Yeongwol Industrial Promotion Agency to determine which Geldart group the LRP and SMP belonged to. Density (g/mL) was calculated using the weight of the sample and occupied volume of the nitrogen gas.

2.7. Contact angle measurement

Contact angle was measured by sessile drop method (Phoenix-150, SEO Co.Ltd, Suwon, Korea) to determine hydrophilicity of particle. To preparation, the particle was spread evenly on the double-side adhesive tape on the glass plate. Then, water drop was placed on the surface with a syringe (Bachmann et al., 2000; Zhao et al., 2018) . After that, the change of contact angle was taken for 450 s at 1 frame per sec, and the angle was analyzed with Image J v.1.52a (Wayne Rasband, National Institutes of Health, Bethesda, MD, USA). Measurements were made at 25 ℃, 35% RH, enclosed room.

2.8. Survivability measurement

Decimal dilution of LRP and granule in sterile 0.85% NaCl solution was spread on the sterile MRS agar plates (Rungsri et al., 2017). After culturing for 48 h at 37 ℃, the resulting colonies were enumerated and expressed as log CFU/g. The survivability was calculated as follows:

$$\text{Survivability} = \frac{(\text{Viability of granule}) \text{x } (\text{the portion of powder in granule})}{\text{Viability of powder}} \text{ x } 100 \qquad (1)$$

The composition ratio of LRP and SMP in granule was applied at the time of initial mixing.

2.9. Microstructure analysis

Particle morphology, bridge formation, surface and structure was observed through scanning electron microscope (Hitachi TM3030Plus tabletop SEM, Tokyo, Japan) at a voltage of 5 kV, 1000 x magnification under high vacuum condition.

1. Mixing

- LRP, SMP (50:50, w/w)
- Impeller speed : 500 rpm
- Mixing time : 5 min

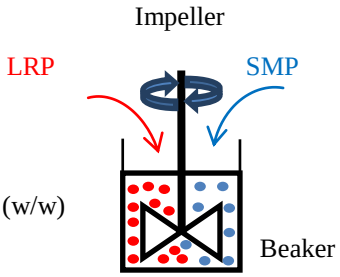

2. Spraying water on the mixture (water fraction = 2.5% (w/w)

3. 2nd mixing

- Impeller speed : 500 rpm
- Mixing time : 5 min

4. Conditioning for 10 min until sufficient reduction of contact angle (Fig 2.2.)

5. Lump removal with 1 mm sieve

Figure 2.1. Moisture-activated dry granulation process

LRP

↓ SMP

Mixture of particles

↓ Moisture-activated dry granulation

Particle aggregates

↓ Fluidized-bed drying (50 ℃)

Dried particle aggregates

↓ Fluidized-bed granulation

Granule

Figure 2.2. Processing steps for granulation of LRP

3. Results and discussion

3.1. Characteristics of powders

The particle size of LRP (9.98 μm) was smaller than SMP (51.73 μm), but the density (1330 kg/m^3) was larger than SMP (1180 kg/m^3); Table 2.1. It is presumed to be due to aggregation of casein protein as a pH decreased during fermentation.

Table 2.1. Properties of LRP and SMP

Powder	$d_{4,3}$, (μm)	True density (kg/m^3)	Geldart group classification
LRP	9.98 ± 0.08	1330 ± 0.00	C
SMP	51.73 ± 1.28	1180 ± 0.00	A

According to the criteria for Geldart group classification, LRP belongs to group 'C' with sized less than 20 μm, less than 1400 kg/m^3 in density, but SMP belongs to group 'A' with sized between 20 to 100 μm, less than 1400 kg/m^3 in density.

In fluidized-bed granulation, LRP belongs to Geldart group 'C' showed not to be fluidized (channeling phenomenon) due to cohesiveness between particles, however SMP belongs to Geldart group 'A' showed good fluidization behavior.

As a result of measuring contact angles of LRP and SMP to water, both of them showed affinity to water (hydrophilicity) and the lowest angle was maintained constantly after 400 s; Figure 2.3. The reason why the LRP had a larger contact angle than SMP was due to aggregation of casein protein by pH dropped during fermentation.

3.2. Effects of SMP addition on fluidized-bed granulation without moisture-activated dry granulation of LRP

To improve the flowability of LRP, well-flowing SMP was mixed at different ratios and then granulated with a fluidized-bed granulator (Table 2.2.). However it was observed that the mixture of 10% SMP did not be fluidized and channeling occurred during granulation. Mixing only 10% of SMP was insufficient to increase the flowability of LRP.

Table 2.2. Particle size before and after granulation of LRP-SMP mixtures

		LRP : SMP (w/w)			
		90 : 10	70 : 30	60 : 40	50 : 50
Particle size ($d_{4,3}$, μm)	Before granulation	11.49 ± 0.10	18.75 ± 0.64	24.86 ± 1.45	33.70 ± 0.96
	After granulation	Not fluidized	95.54 ± 4.11	95.25 ± 8.05	140.50 ± 3.54

On the upper graph of Figure 2.4., before granulation, the smaller sized left peak volume means LRP, the opposite peak volume means SMP. As the mixing ratio of SMP increased, the left peak volume decreased proportionally and the right peak volume increased. However as granulation result, on the down graph of Figure 2.4., the peak volume on the left side drastically reduced, but the peak volume on the right side increased larger and wider. This means particles agglomerated each other and granule formed. Among these granulated results, the mixture of LRP, SMP 50:50 (w/w) showed the largest right peak volume increased (Table 2.4.). This was considered to be the result of the most improved flowability by mixing at half the ratio.

Table 2.3. Particle size and volume fraction of each peak of LRP-SMP mixtures before and after fluidized-bed granulation

		LRP : SMP (w/w)					
		70:30		60:40		50:50	
		before	after	before	after	before	after
$d_{4,3}$ (μm) (volume fraction, %)	Peak 1	7.01 ± 0.01 (24.73 ± 0.34)	2.36 ± 0.99 (4.24 ± 0.09)	-	-	1.76 ± 0.01 (6.73 ± 0.17)	16.01 ± 0.22 (18.39 ± 0.44)
	Peak 2	26.60 ± 0.56 (60.07 ± 0.69)	18.36 ± 0.26 (35.99 ± 0.46)	23.80 ± 0.09 (72.50 ± 1.88)	16.63 ± 0.08 (19.29 ± 0.59)	27.68 ± 0.26 (52.41 ± 1.05)	209.03 ± 1.79 (76.71 ± 0.95)
	Peak 3	79.92 ± 2.31 (5.19 ± 1.00)	370.65 ± 5.62 (59.78 ± 0.38)	95.35 ± 7.94 (27.50 ± 1.88)	233.09 ± 48.70 (80.71 ± 0.59)	111.74 ± 1.25 (40.86 ± 1.22)	487.50 ± 0.51 (4.90 ± 0.51)
Total		18.75 ± 0.64	95.54 ± 4.11	24.86 ± 1.45	95.25 ± 8.05	33.70 ± 0.96	140.50 ± 3.54
Span		4.25 ± 0.15	5.17 ± 0.21	5.24 ± 0.23	2.42 ± 0.11	5.55 ± 0.17	3.49 ± 0.09

Even though a mixture of LRP, SMP 50:50 (w/w) mixture showed good improvement, but particle distribution was broad (span 3.49 ± 0.09) and granule production yield was just 42.82 ± 3.96% (w/w). This was due to the particle loss by entrainment and elutriation of small size, low-density particles (Figure 2.5.). Therefore it showed a wide size distribution curve with irregular granulation and low yield. So additional process with LRP, SMP 50:50 (w/w) mixture was necessary to reduce particle entrainment and elutriation.

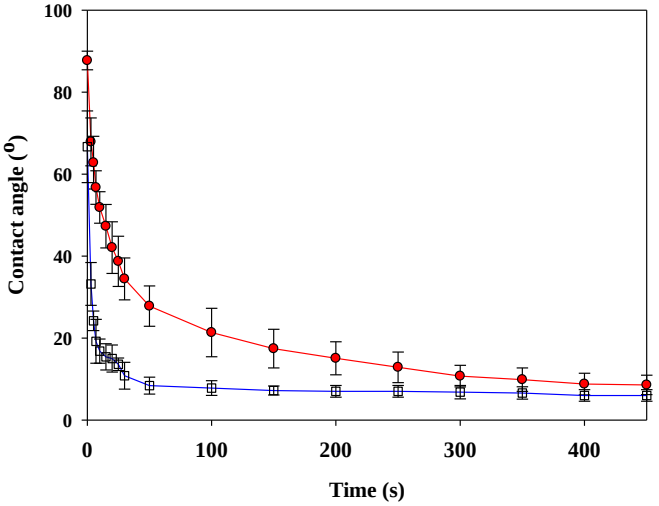

Figure 2.3. Contact angle of LRP (●) and SMP (□) at 35% RH and 25 °C

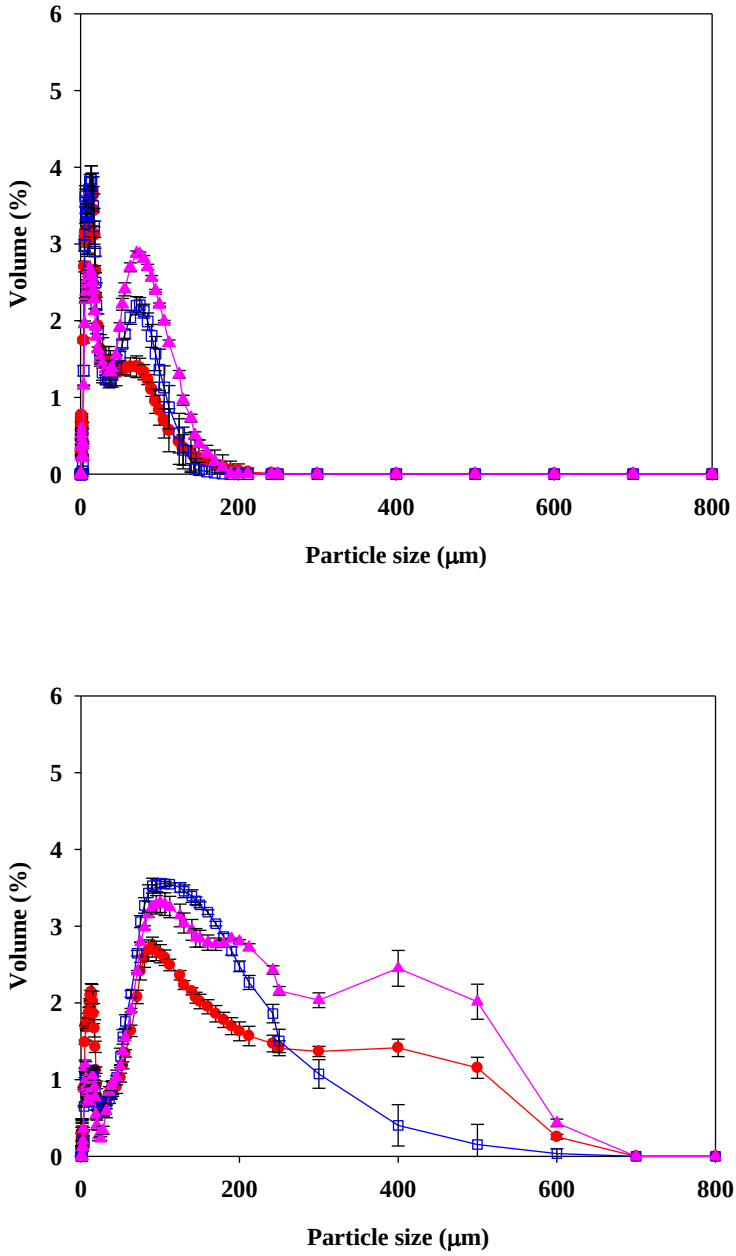

Figure 2.4. Particle size distribution of LRP-SMP mixture before (upper) and after (down) fluidized-bed granulation; LRP : SMP (w/w) = 70:30 (●), 60:40 (□), and 50:50 (▲)

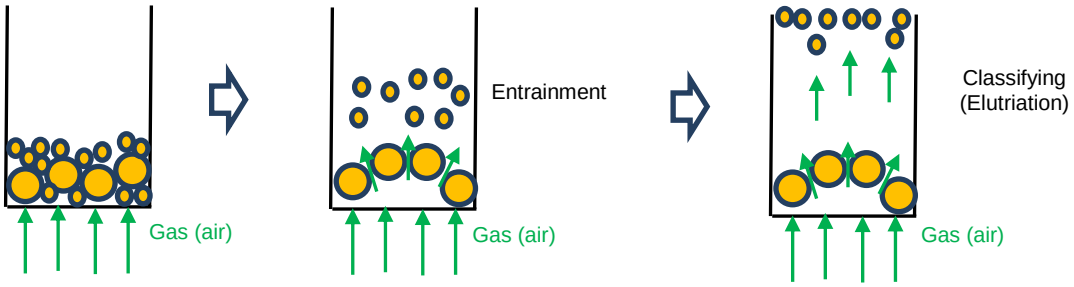

Figure 2.5. Particle elutriation in fluidized-bed

3.3. Effects of moisture-activated dry granulation on fluidized-bed granulation of LRP - SMP mixture

Through moisture-activated dry granulation of LRP, SMP 50:50 (w/w) mixture, small particle size volume (peak 1) consolidated into larger size volume (Figure 2.6; Table 2.4.). This was the result of bridges formed between particles by sprayed water, and because of these bridges, particles linked to each other. In addition, small particles tend to be tacky to adhere by moisture compared to large particles because they have larger surface areas, and have a higher affinity with water due to the difference in Laplace pressure. As a result of this volume change, total particle size $d_{4,3}$ was increased from 33.70 μm to 38.68 μm (Table 2.4.).

Table 2.4. Particle size and volume fraction of each peak of LRP-SMP mixture (50:50, w/w) before and after moisture-activated dry granulation

		LRP – SMP mixture (50:50, w/w)	
		before	After
$d_{4,3}$ (μm) (volume fraction, %)	Peak 1	1.76 ± 0.01 (6.73 ± 0.17)	-
	Peak 2	27.68 ± 0.26 (52.41 ± 1.05)	28.29 ± 0.11 (56.70 ± 1.21)
	Peak 3	111.74 ± 1.25 (40.86 ± 1.22)	119.86 ± 8.53 (43.30 ± 1.21)
Total		33.70 ± 0.96	38.68 ± 1.46
Span		5.55 ± 0.17	3.89 ± 0.06

After moisture-activated dry granulation, followed by fluidized-bed granulation. Granulation increased the total particle size from 38.68 μm to 74.67 μm, but the volume of small particle peak showed a little decrease and large particle peak increased significantly (Figure 2.7; Table 2.5.). The reason why such small particles were not granulated can be explained by the imbibition of binder droplet and capillary force. Through the moisture-activated dry granulation, the pores of particles were partially or fully saturated, thus interfering binder droplet imbibition into pores. Droplet on the particle surface increased binder volume on the surface, also increased bridge volume between particles, so decreased pressure difference between the external and internal pressure of bridge. This decrease in pressure, increased the curvature of the bridge between particles and weaken the capillary force. This reduced capillary force prevented wet granulation in the fluidized-bed.

Table 2. 5. Particle size and volume fraction of each peak of moisture-activated LRP-SMP mixture (50:50, w/w) before and after fluidized-bed granulation

		Moisture-activated LRP-SMP mixture (50:50, w/w)	
		before	After
$d_{4,3}$ (μm) (volume fraction, %)	Peak 1	28.29 ± 0.11 (56.70 ± 1.21)	33.16 ± 0.62 (50.89 ± 2.16)
	Peak 2	119.86 ± 8.53 (43.30 ± 1.21)	64.91 ± 1.04 (7.66 ± 0.69)
	Peak 3	-	289.87 ± 62.79 (41.45 ± 1.47)
Total		38.68 ± 1.46	38.68 ± 1.46
Span		3.89 ± 0.06	6.57 ± 0.33

So an additional process was needed to remove moisture on the surface.

3.4. Effects of dehydration on fluidized-bed granulation of moisture-activated LRP - SMP mixture

Dehydration by fluidized-bed was performed to reduce moisture content on the surface of the particle. As shown in Figure 2.8., moisture content decreased rapidly after 5-min, and then gradually decreased. The water activity was similar to that of moisture content, it decreased until 10-min, and then gradually decreased. In spite of the change of moisture content and water activity, the viable cell count was stable up to 20 min and then started to decrease. The effect of drying on the reduction of viable cell count was consistent with the fact that there is a critical point of moisture content and water activity on the viable cell number reduction. Based on the above results, the drying time 5-min or 10-min were selected as the point where the moisture content and water activity decrease at a stable rate, and then analyzed particle size of each dried particle. The particle size analysis after the 5-min or 10-min drying showed that the size of 10-min dried particle (36.25 μm) was smaller than 5-min dried particle (42.88 μm); Table 2.6. In addition, the volume of the small size peak (56.70%) was rather increased (64.38%) and conversely, the volume of large size peak was decreased from 43.30% to 35.62% after 10-min drying. However, for 5-min drying, the small size peak volume decreased from 56.70% to 49.57%, the large size peak volume increased from 43.30% to 50.43%. This was because dried particles as drying time become longer, that fragmentation occurs due to collision between particles or the wall in the fluidized-bed. This fragmentation phenomenon that occurs in the fluidized-bed is called particle attrition. Eventually, 5-min drying was chosen as the drying time that did not cause particle attrition.

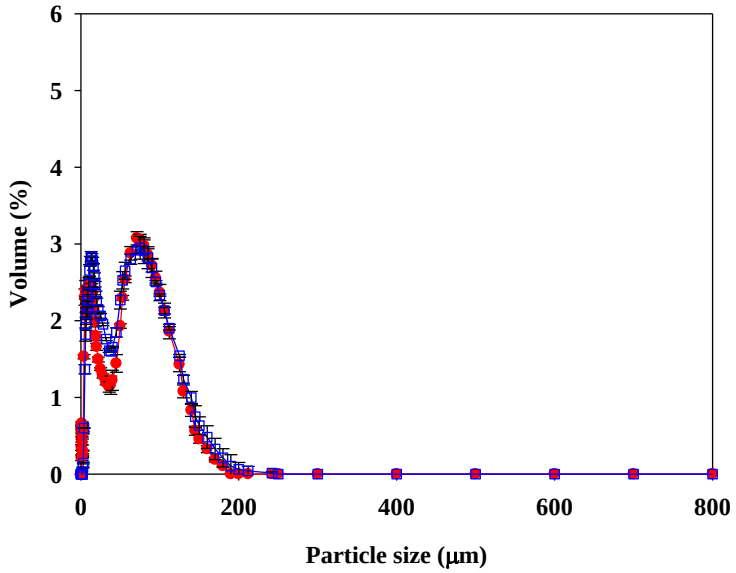

Figure 2.6. Particle size distribution of LRP-SMP mixture (50:50, w/w) before (●) and after (□) moisture-activated dry granulation

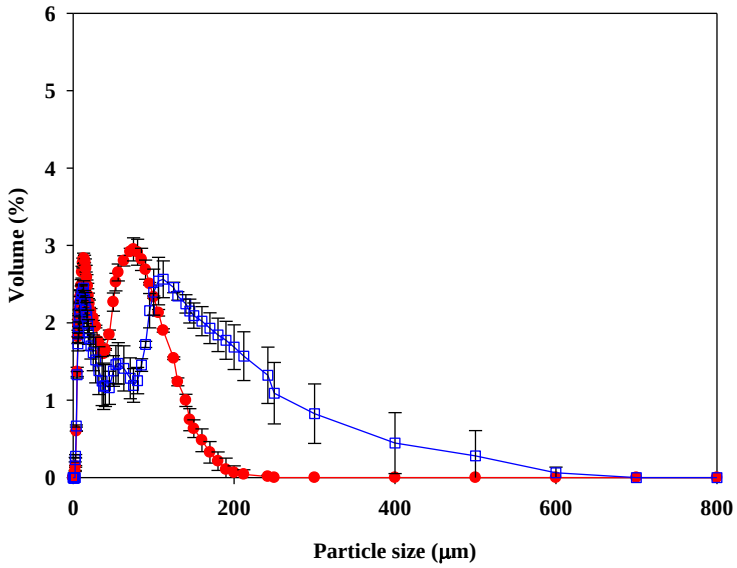

Figure 2.7. Particle size distribution of moisture-activated LRP-SMP mixture (50:50, w/w) before (●) and after (□) fluidized-bed granulation

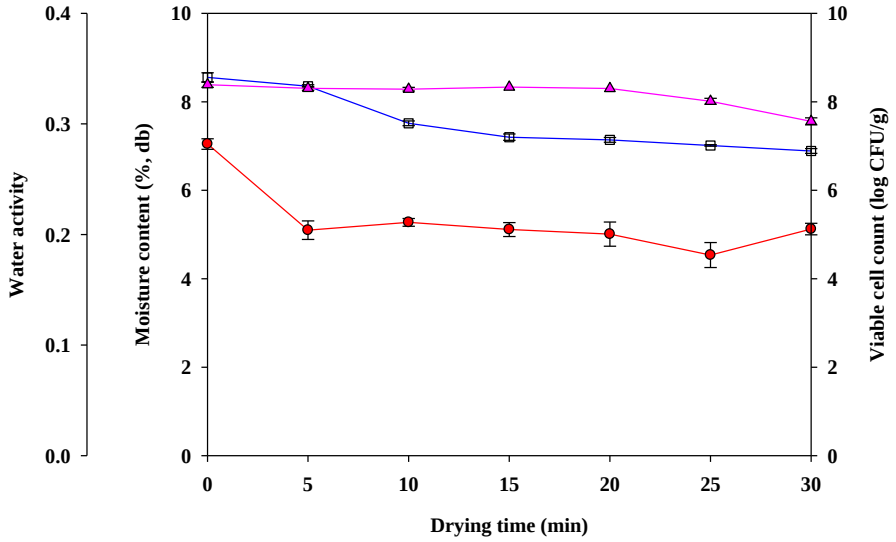

Figure 2.8. Viable cell count (▲), moisture content (●), and water activity (□) of moisture-activated LRP – SMP mixture after dehydration at 50 ℃ for 30 min

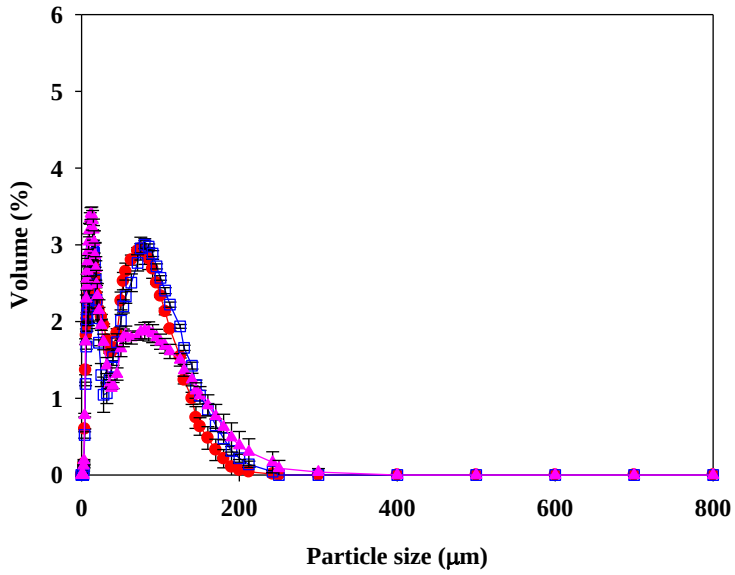

Figure 2.9. Particle size distribution of moisture-activated LRP–SMP mixture before (●) and after dehydration at 50 ℃ for 5 (□) or 10 min (▲)

Table 2.6. Particle size and volume fraction of each peak of moisture-activated LRP-SMP mixture after dehydration at 50 ℃ for 5 or 10 min

		Before dehydration	Moisture-activated LRP-SMP mixture	
			After 5-min dehydration	After 10-min dehydration
$d_{4,3}$ (μm) (volume fraction, %)	Peak 1	28.29 ± 0.11 (56.70 ± 1.21)	19.25 ± 0.35 (49.57 ± 0.38)	26.62 ± 0.26 (64.38 ± 1.33)
	Peak 2	119.86 ± 8.53 (43.30 ± 1.21)	132.31 ± 3.08 (50.43 ± 0.38)	151.24 ± 14.23 (35.62 ± 1.33)
Total		38.68 ± 1.46	42.88 ± 0.48	36.25 ± 2.09
Span		3.89 ± 0.06	4.47 ± 0.07	5.87 ± 0.27

The granulation was carried out using a fluidized-bed with the result of the series procedures described above (mixing in 50:50 w/w, moisture-activated dry granulation, 5-min drying). The granulation operation time was set to 8 or 15 min, and compare the particle size of each (Figure 2.10.). As operation time increased from 8-min to 15-min, the particle size increased from 85.82 to 141.67 μm. In particular, after 15-min of operation, the small size peak volume was significantly reduced and the large size peak volume was greatly increased compared to 8-min.

Table 2.7. Particle size and volume fraction of moisture-activated, dehydrated LRP-SMP mixture before and after fluidized-bed granulation for 8 or 15 min

		Moisture-activated, dehydrated LRP-SMP mixture		
		Before granulation	After 8-min granulation	After 15-min granulation
$d_{4,3}$ (μm) (volume fraction, %)	Peak 1	19.25 ± 0.35 (49.57 ± 0.38)	19.59 ± 0.28 (28.29 ± 0.61)	31.06 ± 0.26 (3.26 ± 0.25)
	Peak 2	132.31 ± 3.08 (50.43 ± 0.38)	310.02 ± 4.41 (71.71 ± 0.61)	301.94 ± 19.60 (96.74 ± 0.25)
Total		42.88 ± 0.48	85.82 ± 1.64	141.67 ± 7.41
Span		4.47 ± 0.07	2.67 ± 0.10	1.68 ± 0.18

The morphology, surface, sintered bridges of the particles were observed through the SEM images (Figure 2.11.). LRP had a very small size with a spherical or elongated shape and the surface had a layered form. The elongated form seemed to be the result of droplet binding together when sprayed in a spray drier. The layer structure of LRP was thought to do the difference in drying rate between the lactose and milk protein at high temperature in a spray drier. However, in the case of SMP, the reason for maintaining the round surface shape was not known precisely because of confidentiality in the producer, but it was

thought to be dried at a relatively low temperature. Granules (granulation in 15-min) had agglomerated structure of LRP, SMP in the form of sintered between SMP and SMP, SMP and LRP, LRP and LRP.

The viable cell count of LGG in granule which had been granulated in 15 min was slightly decreased compared to LRP (before the granulation) from 7.09 to 6.71 log CUF/g (Figure 2.12.). However, considering of SMP was mixed in half, the survival rate of LGG reached 80.22 $\pm$ 0.31%. The loss of LGG was considered to be the result of heat loss and particle loss (by entrainment) containing LGG during fluidized-bed granulation process.

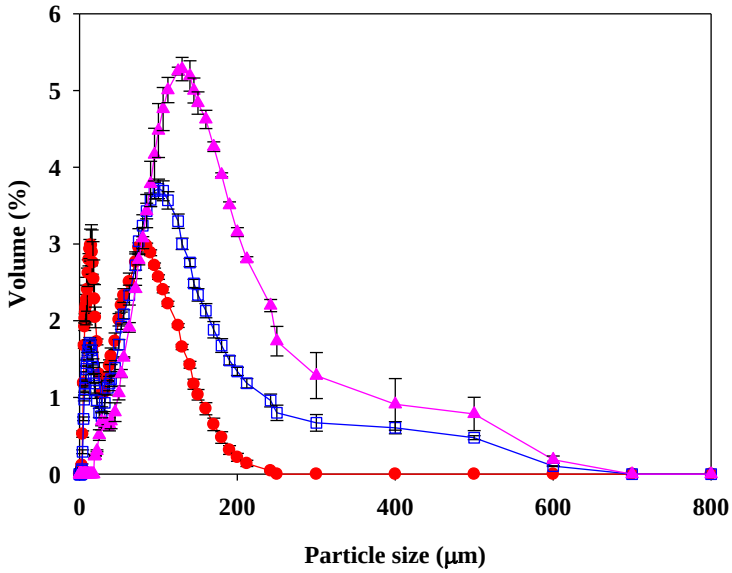

Figure 2.10. Particle size distribution of moisture-activated, dehydrated LRP-SMP mixture before (●) and after fluidized-bed granulation for 8 (□) or 15 (▲) min

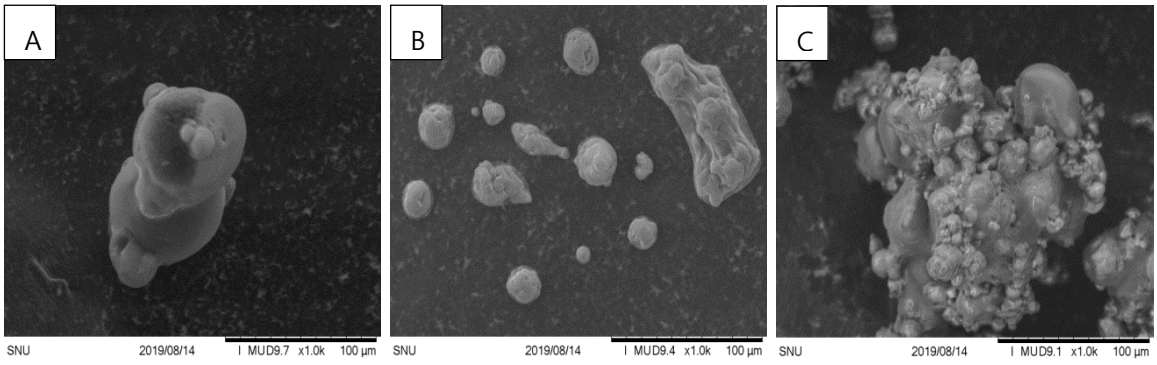

Figure 2.11. SEM images of SMP (A), LRP (B), and granule (C); The granules were prepared by fluidized-bed granulation of moisture-activated, dehydrated LRP – SMP mixture for 15-min

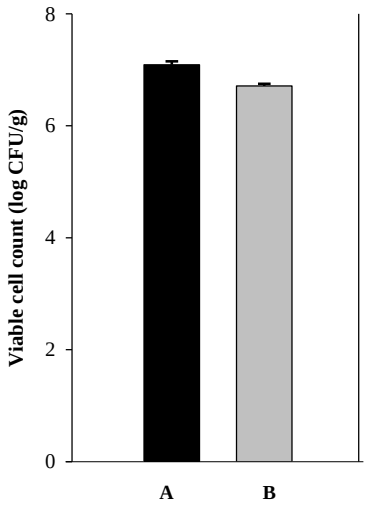

Figure 2.12. Viable cell count : LRP-SMP mixture (50:50 w/w, A) and their granule (15-min granulation, B)

Conclusions

According to Geldart classification of particle, LRP belonged to group ‘C’. Group ‘C’ particle is difficult to be fluidized because of strong attractive force between particles. To fluidize this particle in the fluidized-bed, pre-treatment was carried out in three steps. First, the SMP belongs to group ‘A’ was mixed to reduce the cohesion, thereby increasing the flowability to avoid the channeling phenomenon in the fluidized-bed. As a result, the higher the mixing ratio (50:50 w/w) of SMP, the better the flowability, but occurred loss of small particles by entrainment and irregular granule formed. Second, through surface wetting and liquid bridge formation by moisture-activated dry granulation, small particles integrated into larger particles, which increased total particle size ($d_{4,3}$) up to 14.78%. However wetted surface interfered the imbibition of droplets and weaken the capillary force of liquid bridge between particles. Third, the moisture-activated dry granulation processed particles were dried by the fluidized-bed to remove moisture from the surface. In the case of drying for 10-min, particle attrition occurred, which resulted in a decrease of particle size. Therefore the drying time was chosen as 5-min so that the particle size did not decrease and did not affect the survival of LGG. Granulation was finally performed after three steps processed described above. As granulation operation time was increased from 8 to 15 min, particle size increased proportionally and the distribution maintained relatively narrow state. As a result, through granulation processes, 420% increased in particle size with 60.78 $\pm$ 1.27% (w/w) yield and 80.22 $\pm$ 0.31% cell survivability.

Chapter 3.

Effects of fluidized-bed granulation on the physicochemical properties of particles

1. Introduction

From the previous chapter, LRP (spray-dried LGG encapsulated skim milk) powder was belonged to Geldart group ‘C’ by size and density criteria. These particle characteristics have led to several disadvantages during processing, rehydration, and storage. First, scattering dust due to particle size was very small, causing contamination during the process. Second, difficulty to apply continuous process because of low flowability. Third, due to its strong inter-particle forces, cohesiveness, it formed a lump on the surface when dissolves in water. Fourth, because of the low glass transition temperature, caking occurs depends on storage temperature and humidity. To overcome these disadvantages, attempts were made to form granule by using a conventional fluidized-bed granulator. The granulation was expected to produce the following effects; the flowability was improved by particle size increase, the water penetrated easily into voids between particles during rehydration, prevent the caking phenomenon during storage by reduced surface. However, as mentioned before, because the LRP belongs to the Geldart group ‘C’, it had a strong cohesiveness, so no fluidization occurred in fluidized-bed granulator.

Granulation was performed in serial three steps to make granule. In the first step, skim milk powder belonging to well fluidized Geldart group ‘A’, was mixed with LRP at 50:50 (w/w). However fluidized-bed granulation with mixture resulted in low yield (42.82 $\pm$ 3.96%, w/w), particle size distribution was broad with irregular granulation due to the small size particle entrainment and elutriation in the fluidized-bed granulator. In the second step, the moisture-activated dry granulation process was carried out to reduce these small size particle loss. The moisture-activated dry granulation reduced small size particle entrainment and elutriation by forming bridges between particles. However after moisture-activated dry granulation, the fluidized-bed granulation was inhibited by the high moisture content on the surface, which increased the binder volume and weaken the capillary force of liquid bridge. In the third step, convective drying was performed using a fluidized-bed granulator to reduce the moisture on the surface of particles. And 5 minutes drying was selected which did not cause particle attrition and cell loss. After the three steps above, the final fluidized-bed granulation resulted in a significant increase in particle size, sintered bridges observed through SEM images and a cell survival rate of about 80.22 $\pm$ 0.31%.

In this chapter, the objective of this study was to evaluate the effects of fluidized-bed granulation on the physicochemical properties of particles and assess how much of the disadvantages of the LRP have been overcomed.

2. Materials and methods

2.1. Materials

2.1.1. Spray-dried LGG encapsulated powder (LRP)

LRP was prepared by previously described in section 2.2 and 2.3 of chapter 2.

2.1.2. Fluidization aid

SMP was purchased from Seoul Milk Co.Ltd (Seoul, Korea) and used by a fluidization aid for the fluidized-bed granulation of LRP.

2.1.3. Granules of LRP - SMP mixture

The granules of LRP-SMP mixture were prepared by previously described in section 2.4 of chapter 2 (Figure 3.1.).

2.2. Particle size analysis

The method was previously described in section 2.5 of chapter 2.

2.3. Moisture content measurement

LRP, SMP, and their granule were dried at 105 ℃ in the drying oven for 24 h. By decreased weight, moisture content was expressed in dry basis (X, %) (AOAC, 2005).

$$X\ (\%, \text{db}) = \frac{Moisture\ weight}{Total\ weight - Moisture\ weight} \times 100 \quad (1)$$

2.4. Water activity measurement

The water activity (a_w) of LRP, SMP, and their granule were measured using the Aqualab water activity meter (Decagon, WA, USA) at 25 ℃.

2.5. Dispersibility measurement

After equilibrated at zero a_w (phosphate pentoxide) in a desiccator, one gram of sample was poured into a 50 mL beaker containing 10 mL distilled water and vigorously stirred 25 times for 15 s. The reconstituted solution was then filtered through a 200 μm sieve. And 1 mL of the filtrate was taken and then dried at 105 ℃ for 24 h in the drying oven. After drying, %TS was measured using the change in weight. Thus, dispersibility was measured using the following equation (Balde et al., 2017; Boinrkina et al., 2017; Ji et al., 2016)

$$\% \text{ dispersibility} = \frac{(10+a) \times \%\text{TS}}{a \times \frac{100 - X}{100}} \quad (2)$$

where, a = amount of powder being used, X (%, db) = moisture content in the powder, and %TS = dry matter in percentage in the reconstituted powder after it has been passed through the sieve

2.6. Flowability / cohesiveness measurement

After equilibrated at zero a_w (phosphate pentoxide) in a desiccator, loaded 10 g of sample into a graduated cylinder. The bulk density (ρ_{bulk}) was calculated by occupied volume of particle before tapping. The cylinder was then tapped up and down manually until the volume no longer changed. The tapped density (ρ_{tapped}) was calculated by the occupied volume of the particle after tapped. (Emery et al., 2009; Jinapong et al., 2008). With these measured bulk and tapped density, Carr index (CI) and Hausner ratio (HR) were calculated by the following equations.

$$\text{CI (flowability)} = \frac{(\rho_{\text{tapped}} - \rho_{\text{bulk}})}{\rho_{\text{tapped}}} \text{ x } 100 \quad (3)$$

$$\text{HR (cohesiveness)} = \frac{\rho_{\text{tapped}}}{\rho_{\text{bulk}}} \text{ x } 100 \quad (4)$$

Table 3.1. Classification of powder flowability based on CI value (Carr, 1965).

CI (%)	Flowability
< 15	Very good
15 – 20	Good
20 – 35	Fair
35– 45	Bad
> 45	Very bad

Table 3.2. Classification of powder cohesiveness based on HR value (Hausner, 1967).

HR	Cohesiveness
< 1.2	Low
1.2 – 1.4	Intermediate
> 1.4	High

2.7. Glass transition temperature measurement

After equilibrated at zero a_w (phosphate pentoxide) in a desiccator, Differential Scanning Calorimetry (DSC 250, TA Instrument, New Castle, DE, USA) was used to measure the glass transition temperature. 10 to 15 mg of sample was placed in T zero pan, then hermetically sealed. As a condition, temperature range 2 to 100 ℃, heating rate 10 ℃/min and nitrogen gas flow 50 mL/min for preventing moisture condensation were set (Ozmen et al., 2002).

2.8. Sticky point temperature measurement

After equilibrated at zero a_w (phosphate pentoxide) in a desiccator, Brookfield viscometer (DV3THA, Brookfield Engineering Laboratories, Middleboro, MA, USA) was used with T-F 96 spindle. About 8 g of sample was loaded in cylindrical unit (tapped 10 times) with a water jacket connected to temperature controllable water-bath. The temperature was increased from 20 to 90 ℃ with 10 ℃ intervals, and left for 20 min to stabilization at each temperature. After that, the torques (mN·m) were measured every second for 40 s while the spindle was rotated at 0.3 rpm. The torques (mN·m) of the last 20 s values were averaged. While the torques (mN·m) were measured, the helipath moved up and down at 22.2 mm/min. The sticky point temperature was onset temperature at which the torque changed drastically, and determined by the intersection of the two linear regression lines on the graph (Silalai et al., 2010)

2.9. Statistical analysis

ALL results are presented as mean ± SD. Significant differences were determined by T-test using Sigmaplot version 10.0 (Systat software Inc, San Jose, CA, USA). Differences were determined at $p < 0.05$ and denoted with different superscript.

3. Results and discussion

After the mixing of LRP and SMP at 50:50 (w/w) ratio, the particle size ($d_{4,3}$, μm) increased with each step (Table 3.3.). This was caused by the formation of bridges between the particles by sprayed water in moisture-activated dry granulation, the solidification of the bridge formed in dehydration, and finally granulation in fluidized-bed granulation. The effect of moisture-activated dry granulation, dehydration on the particle size increase was small, but a sharp increase in the fluidized-bed granulation was due to the continuous spraying water and convective drying (Figure 3.3.). Moreover through the fluidized-bed granulation, consolidated two or more peaks integrated into almost one peak in particle size distribution (Figure 3.3.). In addition, except for dehydration step, the span values tended to decrease gradually as the step progressed. In dehydration step, the small particles attached to the large particle surface by water bridge were dried together increased $d_{90,}$ which could be understood in the same context as the result of a larger increase in d_{90} than d_{10}, d_{50} (Table 3.4.).

Table 3.3. Changes in particle size of LRP-SMP mixture during granulation process

Process	$d_{4,3}$ (μm) (volume fraction, %)			Total	Span
	Peak 1	Peak 2	Peak 3		
LRP-SMP mixture	1.76 ± 0.01 (6.73 ± 0.17)	27.68 ± 0.26 (52.41 ± 1.05)	111.74 ± 1.25 (40.86 ± 1.22)	33.70 ± 0.96[a]	5.55 ± 0.17[a]
After moisture-activated dry granulation	-	28.29 ± 0.11 (56.70 ± 1.21)	119.86 ± 8.53 (43.30 ± 1.21)	38.68 ± 1.46[b]	3.89 ± 0.06[b]
After dehydration	-	19.25 ± 0.35 (49.57 ± 0.38)	132.31 ± 3.08 (50.43 ± 0.38)	42.88 ± 0.48[c]	4.47 ± 0.07[c]
After granulation	-	30.06 ± 0.26 (3.26 ± 0.25)	301.94 ± 19.60 (96.74 ± 0.25)	141.67 ± 7.41[d]	1.68 ± 0.18[d]

[abcd] Means in the same column are significantly different (P<0.05).

The reason why the water content of LRP was larger than SMP (Table 3.4.) was that the water was captured due to the aggregated structure formed by fermentation to pH 3.9 below the isoelectric point of casein. Due to this aggregated structure by casein, LRP had a relatively low

Mixing LRP with SMP (50:50)

↓

Moisture-activated dry granulation (water, 2.5% w/w)

↓

Dehydration (50 ℃, 5 min)

↓

Fluidized-bed granulation (50 ℃, 150 L/min, 15-min)

Figure 3.1. Fluidized-bed granulation of LRP - SMP mixture

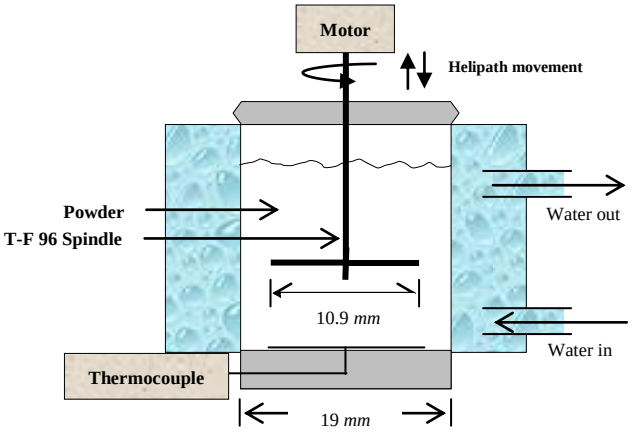

Figure 3.2. Illustration of sticky point temperature measurement using viscometer

water activity even though high water content. The granule showed 7.35% (db) moisture content due to convective co-drying, although the water was sprayed at 0.8 mL/min for 15-min (totally 12 mL, 24% of load mass). However, water activity of granule was higher, because the wetted surface by sprayed water and remained water at the connections between particles.

Table 3.4. Moisture content (X, % db) and water activity (a_w) of SMP, LRP, and their granules

Samples	X (% db)	a_w
SMP	5.75 ± 0.34^{a}	0.34 ± 0.00^{a}
LRP	8.27 ± 0.71^{b}	0.30 ± 0.02^{b}
Granules	7.35 ± 0.32^{c}	0.37 ± 0.00^{c}

[abc] Means in the same column are significantly different (P<0.05).

The SMP was well dispersed in water (Table 3.5.), but the LRP had strong cohesiveness formed lumps on the water surface. This was due to the cohesion between LRP particles due to attractive forces (van der Waals, electrostatic, etc), which results in less space for water molecule to penetrate. However in the case of granule, since the radius of capillary between the particles was larger, the penetration of water molecules became more easier, resulting in an improvement of dispersibility compared to LRP. The improvement of dispersibility due to the increase of capillary diameter between particles can be seen by the following equation of Washburn which calculates liquid penetrating velocity.

$$\frac{\mathrm{d}l}{\mathrm{d}t} = \frac{r}{\eta}\frac{\gamma}{4l}\cos\theta \qquad (5)$$

where, l is length of column of liquid in the capillary (m), t is time (s), r is radius of capillary (m), η is viscosity of liquid (Pa·s), γ is surface tension of liquid (Nm^{-1}), θ is contact angle(°).

Table 3.5. Dispersibility of SMP, LRP, and their granules

Samples	Dispersibility (%)
SMP	95.56 ± 1.37^{a}
LRP	49.68 ± 5.86^{b}
Granules	91.64 ± 2.00^{c}

[abc] Means in the same column are significantly different (P<0.05).

For the smallest size of LRP, the bulk density should be higher than SMP, but the lower value was due to the cohesion of particles (Table 3.6.). But after enough tapping, LRP had the highest

density (tapped density). Due to this cohesiveness, the difference between the bulk and tapped density was large, flowability was bad and cohesiveness was high. However in the case of granule, the surface area was reduced due to the particle granulation, so cohesion was weakened. But although the size of granules larger than SMP, flowability did not improve as much as SMP because the morphology of SMP was close to a round shape, but the granule was an irregular shape (Figure 2.11.).

Table 3.6. Bulk and tapped densities, flowability, and cohesiveness of SMP, LRP, and their granules

Particles	Bulk density	Tapped density	Flowability	Cohesiveness
SMP	0.50 ± 0.01[a]	0.64 ± 0.01[a]	21.17 ± 0.64[a]	1.27 ± 0.01[a]
LRP	0.43 ± 0.00[b]	0.75 ± 0.00[b]	42.86 ± 0.00[b]	1.75 ± 0.00[b]
Granule	0.33 ± 0.00[c]	0.46 ± 0.02[c]	27.42 ± 2.28[c]	1.38 ± 0.04[c]

[abc] Means in the same column are significantly different (P<0.05).

As a result of measuring glass transition temperature using DSC, the temperature was higher in order of SMP, granule, LRP (Table 3.7.). In particular, the glass transition temperature of granule consisting of SMP and LRP, were present between the glass transition temperature of SMP and LRP (Figure 3.4.).

The fractions of each constituent in the granule can be derived using the Couchmann and Karasz (1978, eq 6) equation, which is an extension of Gordon and Taylor (1952) equation.

$$T_{gm} = \frac{w_1 T_{g1} + \left(\frac{\Delta C_{p2}}{\Delta C_{p1}}\right) w_2 T_{g2}}{w_1 + \left(\frac{\Delta C_{p2}}{\Delta C_{p1}}\right) w_2} \quad (6)$$

Where T_{gm} is the glass transition temperature of granule, w_i is mole fraction of component *i*, T_{gi} is the glass transition temperature of component i, ΔC_{pi} is the change of heat capacity of component *i* between the glass and rubbery states. Through substituting the T_g and ΔC_p data of Table 3.7. into the Couchmann and Karasz equation, the fraction of SMP was about 1.08 times more than LRP in the granule.

Table 3.7. Moisture content (*X*), glass transition temperature (T_g), change of specific heat capacity (ΔC_p) and sticky point temperature (T_s) of SMP, LRP, granule conditioned at zero a_w

Sample	X (%, db)	T_g (°C)	Onset T_g (°C)	Endset T_g (°C)	ΔC_p (J/g°C)	T_S (°C)
SMP	3.27 ± 0.13[a]	75.06 ± 0.23[a]	73.62 ± 0.44	76.95 ± 0.61	0.54 ± 0.06[a]	88.65 ± 1.04[a]
LRP	5.08 ± 0.28[b]	64.16 ± 0.80[b]	60.80 ± 1.00	67.05 ± 0.59	0.57 ± 0.00[a]	78.46 ± 1.98[b]
Granules	4.07 ± 0.20[c]	69.67 ± 0.35[c]	67.21 ± 0.09	72.32 ± 0.59	0.62 ± 0.02[a]	85.98 ± 3.98[c]

[abc] Means in the same column are significantly different (P<0.05).

Sticky point temperature resulted in 88.65 ± 1.04[a] ℃ of SMP, 78.46 ± 1.98 ℃[b] of LRP and 85.98 ± 3.98[a,b] ℃ of granule ($p<0.05$), showed sticky temperature of granule also between SMP and LRP, like glass transition temperature (Table 3.7.).

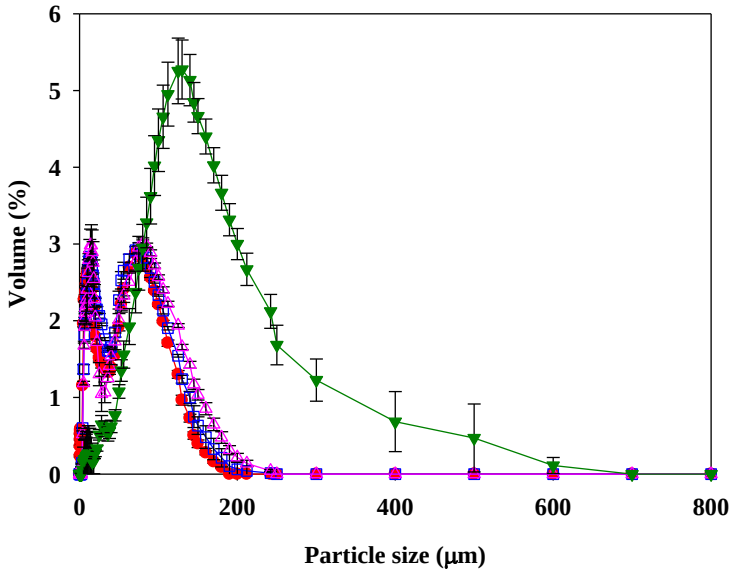

Figure 3.3. Particle size distribution of LRP-SMP mixture (50:50, w/w) : LRP-SMP mixture (●), after moisture-activated dry granulation (□), after dehydration (△), and after granulation (▼)

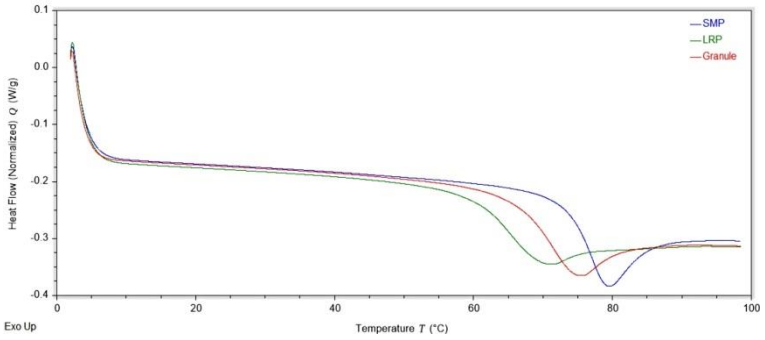

Figure 3.4. DSC heat flow curve of SMP, LRP, and their granules conditioned at zero a_w

4. Conclusions

Several processes for fluidized-bed granulation had increased the particle size of LRP and SMP mixture from 33.70 μm to 141.67 μm (420%). In particle size distribution, granule showed an almost mono-modal peak with the lowest span value. In spite of the continuous water spraying during granulation, the convective drying was carried out simultaneously, resulting in 7.35% moisture content (dry basis) and 0.37 water activity.

This granule showed a higher degree of dispersibility upon rehydration in water than LRP. In addition, the granule has reduced cohesiveness and improved flowability compared to LRP. Under zero water activity condition, the glass transition and sticky point temperature of granule were located between the glass transitions of SMP, LRP. By using Couchmann and Karasz equation, the composition ratio of SMP, LRP in granule could be calculated to 1.08 : 1 (SMP : LRP).

References

Aureli, P., Capurso, L., Castellazzi, A. M., Clerici, M., Giovannini, M., Morelli, L., Zuccotti, G. V. (2011). Probiotics and health: An evidence-based review. *Pharmacological Research, 63*(5), 366-376.

Bachmann, J., Horton, R., Van Der Ploeg, R. R., & Woche, S. (2000). Modified sessile drop method for assessing initial soil-water contact angle of sandy soil. *Soil Science Society of America Journal, 64*(2), 564-567. <Go to ISI>://WOS:000089446200017.

Bhandari, B. R., & Howes, T. (1999). Implication of glass transition for the drying and stability of dried foods. *Journal of Food Engineering, 40*(1-2), 71-79.

Bhattacharjee, S., Chakraborty, P., Jana, M., Das, R., Ganguly, D. (2016). Recent trends in granulation techniques: A technical review. *World Journal of Pharmacy and Pharmaceutical Sciences, Vol 5, Issue 9*, 434-454.

Burgain, J., Gaiani, C., Cailliez-Grimal, C., Jeandel, C., & Scher, J. (2013). Encapsulation of *Lactobacillus rhamnosus* GG in microparticles: Influence of casein to whey protein ratio on bacterial survival during digestion. *Innovative Food Science & Emerging Technologies, 19*, 233-242.

Burgain, J., Gaiani, C., Linder, M., & Scher, J. (2011). Encapsulation of probiotic living cells: From laboratory scale to industrial applications. *Journal of Food Engineering, 104*(4), 467-483.

Burgain, J., Scher, J., Lebeer, S., Vanderleyden, J., Cailliez-Grimal, C., Corgneau, M., Gaiani, C. (2014). Significance of bacterial surface molecules interactions with milk proteins to enhance microencapsulation of *Lactobacillus rhamnosus* GG. *Food Hydrocolloids, 41*, 60-70.

Capurso, L. (2019). Thirty Years of *Lactobacillus rhamnosus* GG: A Review. *J Clin Gastroenterol, 53 Suppl 1*, S1-S41.

Chavarri, M., Maranon, I., Villaran, M. C. (2012). Encapsulation Technology to Protect Probiotic Bacteria. *INTECH*, http://dx.doi.org/10.5772/50046

Corcoran, B. M., Ross, R. P., Fitzgerald, G. F., & Stanton, C. (2004). Comparative survival of probiotic lactobacilli spray-dried in the presence of prebiotic substances. *Journal of Applied Microbiology, 96*(5), 1024-1039.

Couchman, P. R. and Karasz, F. E. (1978). A Classical Thermodynamic Discussion of the Effect of Composition on Glass-Transition Temperatures. *American Chemical Society, Vol. 11, No 1, January-February 1978.*

De Prisco, A., & Mauriello, G. (2016). Probiotication of foods: A focus on microencapsulation

tool. *Trends in Food Science & Technology, 48*, 27-39.

Ding, W. K., & Shah, N. P. (2007). Acid, bile, and heat tolerance of free and microencapsulated probiotic bacteria. *Journal of Food Science, 72*(9), M446-M450.

Geldart, D. (1973). Types of Gas Fluidization. *Powder Technology, 7*(5), 285-292.

Gorbach, S., Doron, S., Magro, F. (2017). *Lactobacillus rhamnosus* GG, *The Microbiota in Gastrointestinal Pathophysiology*, *Chapter 7*, 79-88

Guerin, J., Bacharouche, J., Burgain, J., Lebeer, S., Francius, G., Borges, F., Gaiani, C. (2016). Pili of *Lactobacillus rhamnosus* GG mediate interaction with beta-lactoglobulin. *Food Hydrocolloids, 58*, 35-41.

Guerin, J., Petit, J., Burgain, J., Borges, F., Bhandari, B., Perroud, C., Gaiani, C. (2017). *Lactobacillus rhamnosus* GG encapsulation by spray-drying: Milk proteins clotting control to produce innovative matrices. *Journal of Food Engineering, 193*, 10-19.

Huang, S., Vignolles, M. L., Chen, X. D., Le Loir, Y., Jan, G., Schuck, P., & Jeantet, R. (2017). Spray drying of probiotics and other food-grade bacteria: A review. *Trends in Food Science & Technology, 63*, 1-17.

Joshi, S., Kamat, R. (2017). To study and understand the process of wet granulation by fluidized-bed granulation technique. *International Journal of Research in Pharmacy and Chemistry*, *7*(3), 232-238.

Julklang, W., Golman, B. (2014). Analysis of slurry drying in a spray dryer. *International Journal of Engineering and Technology*. *Vol 5, No 6, Dec 2013-Jan 2014.*

Kim, S. W., Park, K. Y., Kim, B., Kim, E., & Hyun, C. K. (2013). *Lactobacillus rhamnosus* GG improves insulin sensitivity and reduces adiposity in high-fat diet-fed mice through enhancement of adiponectin production. *Biochemical and Biophysical Research Communications, 431*(2), 258-263.

Lam, E. K. Y., Tai, E. K. K., Koo, M. W. L., Wong, H. P. S., Wu, W. K. K., Yu, L., Cho, C. H. (2007). Enhancement of gastric mucosal integrity by *Lactobacillus rhamnosus* GG. *Life Sciences, 80*(23), 2128-2136.

Liu, Y. D., Kimura, S. (1993). Fluidization and entrainment of difficult-to-fluidize fine powder mixed with easy-to-fluidize large particles. *Powder Technology 75*, 189-196.

Liu, B., Fu, N., Woo, M. W., & Chen, X. D. (2018). Heat stability of *Lactobacillus rhamnosus* GG and its cellular membrane during droplet drying and heat treatment. *Food Research International, 112*, 56-65.

Martin, M. J., Lara-Villoslada, F., Ruiz, M. A., & Morales, M. E. (2015). Microencapsulation of bacteria: A review of different technologies and their impact on the probiotic effects.

Innovative Food Science & Emerging Technologies, 27, 15-25.

Martini, L. G., Avontuur, P., George, A., Willson, R. J., & Crowley, P. J. (1999). Solubility parameter and oral absorption. *European Journal of Pharmaceutics and Biopharmaceutics, 48*(3), 259-263.

Mezhericher, M., Levy, A., & Borde, I. (2008). Modelling of particle breakage during drying. *Chemical Engineering and Processing-Process Intensification, 47*(8), 1410-1417.

Mezhericher, M., Levy, A., & Borde, I. (2012). Three-Dimensional Spray-Drying Model Based on Comprehensive Formulation of Drying Kinetics. *Drying Technology, 30*(11-12), 1256-1273.

Moayyedi, M., Eskandari, M. H., Rad, A. H. E., Ziaee, E., Khodaparast, M. H. H., & Golmakani, M. T. (2018). Effect of drying methods (electrospraying, freeze drying and spray drying) on survival and viability of microencapsulated *Lactobacillus rhamnosus* ATCC 7469. *Journal of Functional Foods, 40*, 391-399.

Nag, A., Waterland, M., Janssen, P., Anderson, R., & Singh, H. (2019). Importance of intact secondary protein structures of cell envelopes and glass transition temperature of the stabilization matrix on the storage stability of probiotics. *Food Research International, 123*, 198-207.

Orlando, A., Linsalata, M., Notarnicola, M., Tutino, V., & Russo, F. (2014). *Lactobacillus* GG restoration of the gliadin induced epithelial barrier disruption: the role of cellular polyamines. *Bmc Microbiology, 14*.

Ozmen, L., & Langrish, T. A. G. (2002). Comparison of glass transition temperature and sticky point temperature for skim milk powder. *Drying Technology, 20*(6), 1177-1192. <Go to ISI>://WOS:000176742200007.

Papizadeh, M., Nahrevanian, H., Rohani, M., Hosseini, S. N., Shojaosadati, S. A. (2016). *Lactobacillus rhamnosus* Gorbach-Gordin (GG): A Top Well-Researched Probiotic Strain. *J Med Bacteriol*. *Vol. 5, No. 5*, pp.44-59

Patil, N., Khadse, S. C. and Ige, P. P. (2016). Review on novel granulation techniques. *World Journal of Pharmaceutical Research, Vol 5, Issue 7.*

Pitigraisorn, P., Srichaisupakit, K., Wongpadungkiat, N., & Wongsasulak, S. (2017). Encapsulation of *Lactobacillus acidophilus* in moist-heat-resistant multilayered microcapsules. *Journal of Food Engineering, 192*, 11-18.

Pont, V., Saleh, K., Steinmetz, D., & Hemati, M. (2001). Influence of the physicochemical properties on the growth of solid particles by granulation in fluidized-bed. *Powder Technology, 120*(1-2), 97-104.

Porowska, A., Dosta, M., Fries, L., Gianfrancesco, A., Heinrich, S., & Palzer, S. (2016). Predicting the surface composition of a spray-dried particle by modelling component reorganization in a drying droplet. *Chemical Engineering Research & Design, 110*, 131-140.

Quinto, E. J., Jimenez, P., Caro, I., Tejero, J., Mateo, J., Girbes, T., (2014). Probiotic Lactic Acid Bacteria: A review. *Food and Nutrition Sciences, 5*, 1765-1775

Rungsri, P., Akkarachaneeyakorn, N., Wongsuwanlert, M., Piwat, S., Nantarakchaikul, P., & Teanpaisan, R. (2017). Effect of fermented milk containing *Lactobacillus rhamnosus* SD11 on oral microbiota of healthy volunteers: A randomized clinical trial. *Journal of Dairy Science, 100*(10), 7780-7787. <Go to ISI>://WOS:000410876600003.

Schell, D., & Beermann, C. (2014). Fluidized-bed microencapsulation of *Lactobacillus reuteri* with sweet whey and shellac for improved acid resistance and in-vitro gastro-intestinal survival. *Food Research International, 62*, 308-314.

Schuck, P., Dolivet, A., Mejean, S., Herve, C., & Jeantet, R. (2013). Spray drying of dairy bacteria: New opportunities to improve the viability of bacteria powders. *International Dairy Journal, 31*(1), 12-17.

Semyonov, D., Ramon, O., Kovacs, A., Friedlander, L., & Shimoni, E. (2012). Air-Suspension Fluidized-Bed Microencapsulation of Probiotics. *Drying Technology, 30*(16), 1918-1930.

Serrazanetti, D. I., Gottardi, D., Montanari, C., Gianotti, A. (2013). Dynamic Stresses of Lactic Acid Bacteria Associated to Fermentation Processes. *INTECH*. http://dx.doi.org/10.5772/51049

Silalai, N., & Roos, Y. H. (2010). Roles of Water and Solids Composition in the Control of Glass Transition and Stickiness of Milk Powders. *Journal of Food Science, 75*(5), E285-E296.

Shanmugam, S. (2015). Granulation techniques and technologies: recent progresses. *BioImpacts, 5*(1), 55-63.

Thejaswini, P., Suguna, B., Sumalatha, N., Umasankar, K., Reddy, P. J. (2013). Advanced granulation techniques for pharmaceutical formulations-overview. *International Journal of Research in Pharmaceutical and Nano Sciences*. *2*(6), 723-732.

Tomas, J., & Kleinschmidt, S. (2009). Improvement of Flowability of Fine Cohesive Powders by Flow Additives. *Chemical Engineering & Technology, 32*(10), 1470-1483.

Tripathi, P., Beaussart, A., Alsteens, D., Dupres, V., Claes, I., von Ossowski, I., Dufrene, Y. F. (2013). Adhesion and Nanomechanics of Pili from the Probiotic *Lactobacillus*

rhamnosus GG. *Acs Nano, 7*(4), 3685-3697.

Vehring, R., Foss, W. R., & Lechuga-Ballesteros, D. (2007). Particle formation in spray drying. *Journal of Aerosol Science, 38*(7), 728-746.

Yan, F., Polk, D. B. (2012). *Lactobacillus rhamnosus* GG: An Updated Strategy to Use Microbial Products to Promote Health. *Funct Food Rev. 4*(2), 77-84

Ying, D. Y., Phoon, M. C., Sanguansri, L., Weerakkody, R., Burgar, I., & Augustin, M. A. (2010). Microencapsulated *Lactobacillus rhamnosus* GG Powders: Relationship of Powder Physical Properties to Probiotic Survival during Storage. *Journal of Food Science, 75*(9), E588-E595.

Ying, D. Y., Sanguansri, L., Weerakkody, R., Bull, M., Singh, T. K., & Augustin, M. A. (2016). Effect of encapsulant matrix on stability of microencapsulated probiotics. *Journal of Functional Foods, 25*, 447-458.

Zhao, T. Y., & Jiang, L. (2018). Contact angle measurement of natural materials. *Colloids and Surfaces B-Biointerfaces, 161*, 324-330. <Go to ISI>://WOS:000423636100039.

Zheng, X. F., Fu, N., Duan, M. L., Woo, M. W., Selomulya, C., & Chen, X. D. (2015). The mechanisms of the protective effects of reconstituted skim milk during convective droplet drying of lactic acid bacteria. *Food Research International, 76*, 478-488.

Zhou, Tao., Li, Hongzhong. (1999). Effects of adding different size of particles on fluidization of cohesive particles. *Powder Technology, Volume 102, Issue 3*, 215-220.

국 문 초 록

현대인들은 다양한 건강기능성을 갖춘 프로바이오틱스를 일상에서 손쉽게 섭취하고있다. 하지만 이러한 섭취는 주로 액상이나 분말형태로 섭취하고있는데 이중 분말 형태는 다루기가 쉽고, 복용하기도 용이하며 장기간 보관이 가능하다는 장점을 지닌다. 그러나 이러한 분말은 주로 동결건조 방법으로 제작되다보니 시중에 판매되고 있는 프로바이오틱스의 단가는 비싼 편이다. 이에 단가를 낮추기위해 상대적으로 저렴한 분무건조방법이 많이 연구되었다. 하지만 분무건조 방식으로 생산되는 분말은 사이즈가 매우 작다보니 입자간의 응집력이 강해서 흐름성이 낮고, 재수화 시 덩어리를 형성하며, 저장 중 케이킹 현상을 발생시킨다. 이러한 단점을 극복하기 위해 과립을 형성하는 방안이 많이 시도되어왔다. 과립화 방안 중에서 유동층 과립기의 경우 열 전도도가 높고 과립의 생성과 건조가 거의 동시에 이루어져 효율성이 높다는 장점을 지니고 있다. 하지만 이러한 유동층 과립기를 이용한 과립의 방법은 작은 입자를 지닌 분말의 경우 마찬가지로 응집력이 강해서 유동화가 어렵다는 단점이 있고 더욱이 프로바이오틱스가 포집된 분말의 경우 건조 온도를 높게 설정할 수 없다는 약점을 지니고 있다.

그래서 본 연구에서는 분무건조로 형성된 프로바이오틱스 분말을 유동층 과립기를 이용, 유동화를 위한 다른 분말과의 혼합 및 수분 활성 건조 과립 방법과 병행하여 과립화를 하고자하였다. 그리고 과립화를 통해 앞서 설명한 단점들이 얼마나 극복되었는지를 확인하기위해 입자의 물리화학적 변화를 추적하였다.

먼저 *Lactobacillus rhamnosus* GG가 포집된 분무건조 분말을 확보하기위해 탈지분유 10% (w/w), 포도당 2% (w/w), 효모추출물 1% (w/w)를 포함한 배지에 LGG 균을 배양한 후 분무건조를 위한 점착방지물 (탈지분유)을 일정부분 추가하여 분무건조를 실시하였다. 앞서 설명한대로 분무건조된 분말은 입자가 작고 응집성이 있기 때문에 유동층 과립기에서 유동화가 되지않아서 유동화가 잘 이루어지는 탈지분유를 10%, 30%, 40%, 50% (w/w) 비율로 혼합하여 유동층 건조기로 과립을 하고자하였다. 그 결과 50% 혼합한 혼합물의 입도크기 변화가 가장 크게 나타났으나 입도크기 분포가 넓고(사이즈가 다양), 수율이 42.8% (w/w)에 그쳤다. 이는 유동층 과립기 내에서 사이즈가 작고 밀도가 낮은 분말이 기류에 의해 공중으로 이송되면

서 생기는 층 분리 현상 때문이다. 그래서 작은 입자의 이송을 감소시키기위해 수분 활성 건조 과립화 방법을 사용하였다. 이는 탈지분유 50%가 포함된 혼합물에 물 2.5% (w/w)를 분사한 후 임펠러로 혼합하는 방식으로 진행되었으며, 그 결과 입도분포에서 작은 사이즈를 지닌 입자 부피가 감소 (6.73%)하는 것을 확인하였다. 이렇게 형성된 수분 활성 건조 과립화된 혼합물은 유동층 과립기에서 과립화 결과 작은 입자의 경우 과립화가 지연되었는데 이는 입자 표면에 수분 부피가 증가되어 과립화에 방해요인으로 작용했기 때문이다. 그래서 입자 표면의 수분을 제거하기위해 유동층 과립기를 이용하여 건조공정을 진행하였으며 실험을 통해 5분 건조시 입자의 분열이나 셀의 손실을 방지할 수 있다고 결론내었다. 결국 탈지분유 50% (w/w) 혼합물은 수분 활성 건조 과립화 방법 및 건조 공정을 거쳐 유동층 과립기에서 과립화가 진행되었으며 공정시간 8-min과 15-min 동안 진행한 결과 과립화를 통한 입자 크기의 증가(33.70 μm에서 각각 85.82 μm, 141.67 μm)가 이루어졌으며 크기 증가는 공정시간에 비례하는 것을 확인하였다. 또한 입도크기 분포는 거의 단봉형으로 형성되었고 셀 생존율은 80.22%, 수율은 60.78% (w/w)로 상승하였다. 과립의 형성모양은 전자주사현미경을 통해 포도알과 같이 형성되었음을 확인하였다.

이러한 과립의 형성이 물리화학적으로 어떠한 변화를 유발하는 지를 확인하기 위해 수분함량, 수분활성도, 분산성, 흐름성 / 응집성, 유리전이온도, 점착온도를 측정하였다. 이 중에서 수분함량, 수분활성도는 생성된 직후에 측정하였으나, 나머지 척도는 수분의 영향을 배제하기위해 오산화인을 포함한 데시케이터에서 25도에서 수분활성도 0.0의 평형을 이룬 입자를 사용하여 측정하였다. 그 결과 수분함량과 수분활성도에서 과립은 유동층 과립기에서 15-min동안 수분이 분무 (중량의 24%)되었음에도 불구하고 대류건조가 동시에 발생하는 특성으로 인해 원물 (분무건조 분말, 탈지분유)에 비해 크게 증가되지않았다. 그리고 물에 분산성에 있어 분무건조 분말은 49.68%임에 반해 과립은 91.64%로 크게 증가하였는데 이는 과립의 구조로 인한 공극 크기의 증가와 함께 포함된 탈지분유의 분산성 (95.56%)에 기인한 것으로 판단된다. 흐름성과 응집성에 있어 분무건조 분말은 측정결과 흐름성이 나쁘고 응집성은 높게 측정되었는데 탈지분유는 둘다 양호로 측정되었다. 과립의 경우 흐름성과 응집성이 모두 보통으로 개선되었다. 이러한 과립의 개선은 입자의 크기가 증가됨에서 기인하였으나 탈지분유만큼의 개선이 이루어지지않은 것은 탈지분유는

둥근 모양을 지니고 있는데 반해, 과립은 무정형의 형태(전자주사현미경)이기때문으로 판단된다. 저장 중 케이킹을 형성하는데 중요한 요인인 유리전이온도 측정결과 과립은 분무건조 분말 (64.16 ℃)과 탈지분유 (75.06 ℃)의 중간지점인 69.76 ℃인 것으로 나타났으며 함께 측정된 유리전이시 열용량의 변화를 이용하여 코치만 및 카라즈 방정식을 이용하여 과립의 형성 분율을 계산하였다. 계산결과 과립에서 탈지분유와 분무건조 분말의 분율은 1.08:1로 나타났다. 점착온도의 경우 분무건조 분말, 탈지분유 및 과립에서 각각 83.15 ℃, 78.46 ℃, 85.98 ℃로 측정되었다. 과립의 점착온도는 분무건조 분말과 탈지분유의 그것 사이에 나타났으며, 기계적인 강제 교반에 의한 측정방식 및 분무건조 분말 및 탈지분유의 혼합으로 인해 편차가 크게 나타난 것으로 판단된다.

결과적으로 분무건조 분말은 탈지분유와 혼합할 경우 유동층 과립기에서 과립화가 가능하였으나 낮은 수율과 불규칙한 과립형성으로 인하 수분 활성 건조 과립화 및 건조 공정이 추가로 필요하였다. 하지만 이렇게 형성된 과립의 경우 향상된 수율과 높은 셀 생존율을 보였다. 게다가 분산성, 흐름성의 개선 및 응집성의 감소를 가져왔으며 유리 전이 및 접착점 온도도 상승시킬 수 있었다. 이러한 결과를 바탕으로 LGG가 포집된 분무건조 탈지분유 분말의 경우 유동층 건조기에서 과립화가 가능하며 이러한 과립화를 통해 여러가지 단점을 극복할 수 있다고 판단된다.